Politecnico di Torino

Master's degree in biomedical engineering
A.Y. 2023/2024
Session of July 2024

Characterization of a vitrimer with methacrylate cellulose crosslinker for 3D printing

Relatore:
Prof. Ignazio Roppolo

Candidata:
Sara Bergia

INDEX

ABSTRACT **1**

CHAPTER 1: INTRODUCTION AND AIM OF THE WORK **2**

CHAPTER 2: CANS AND VITRIMERS **4**

2.1 VITRIMERS PROPERTIES 6

2.2 DYNAMIC TRANSESTERIFICATION REACTIONS 9

2.3 BIOBASED VITRIMERS 10

2.3.1 VITRIMERS FROM BIOBASED AROMATIC PRECURSORS 10

2.3.2 VITRIMERS FROM BIOBASED ALIPHATIC PRECURSORS 12

2.4 BIOMEDICAL APPLICATION 15

CHAPTER 3: 3D PRINTING **16**

3.1 PHOTOPOLYMERIZATION-BASED TECHNIQUES 17

3.1.1 DPL: MECHANISM AND CHARACTERISTICS 19

3.2 3D PRINTING FORMULATIONS 21

CAPITOLO 4: MATERIALS AND METHODS **24**

4.1 MATERIALS FOR 3D PRINTING 24

4.2 PREPARATION OF 3D PRINTING FORMULATION AND PRINTING PROCEDURE 26

4.2.1. SYNTHESIS OF METHACRYLATE CELLULOSE 26

4.2.2 FORMULATION'S PREPARATION 26

4.2.3 PRINTING PROCEDURE 27

4.2.4 HEAT TREATMENT 28

4.3 CHARACTERIZATION METHODS 28

4.3.1 RHEOLOGY AND PHOTORHEOLOGY 29

4.3.2 STRESS RELAXATION 31

4.3.3 SWELLING AND GEL PERCENTAGE TEST 31

4.3.4 DIFFERENTIAL SCANNING CALORIMETRY ANALYSYS (DSC) 32

4.3.5 FTIR-ATR SPECTROSCOPY 33

4.3.6 MECHANICAL CHARACTERIZATION 33

4.3.7 SELF-HEALING TEST 34

4.3.8 3D SCANNER 35

CHAPTER 5: RESULTS AND DISCUSSION **36**

5.1 RHEOLOGY AND PHOTORHEOLOGY: CHOICE OF THE BEST FORMULATION 36

5.2 STRESS RELAXATION 39

5.3 SWELLING AND GEL CONTENT TEST 40

5.4 DSC 41

5.5 FTIR-ATR SPECTROSCOPY 44
5.6 TENSILE TEST 48
5.7 SELF HEALING TEST 50
5.8 3D SCANNER 52
5.9 BIOMEDICAL APPLICATIONS OF THE MATERIAL 53
CHAPTER 6: CONCLUSION 55
REFERENCES 57

ABSTRACT

In the biomedical industry, polymers have been a real revolution due to their adjustable physicochemical properties and possibilities for biological functionalization, suitable for a wide range of applications. Depending on their chemical structure, they are divided into three macrocategories: thermoplastic polymers, hydrogels, and thermosetting polymers. The latter are often used because of their excellent mechanical and thermal properties, good fatigue and creep resistance, and ease and speed of production. However, because of the irreversible chemical bonds created during the curing process, thermosets are inherently insoluble and infusible, making them particularly problematic in the recycling stage. For this reason, in recent decades, work has begun on a family of innovative polymers called CANs, which are formed from adaptable covalent networks capable of remolding due to external stimuli such as light or heat. This makes CANs materials with mechanical properties similar to thermoset polymers, but with recycling capabilities comparable to thermoplastic polymers. In 2011, Leibler and coworkers enriched this field by introducing the concept of vitrimers, cross linked polymers in which covalent bonds can be redistributed within the network upon heating by associative exchange reactions, maintaining the integrity of the network. Since this seminal work, many research groups have begun to work on the theoretical backgroung of vitrimers, discovering new features such as shape memory, self-healing, and stimulus response. Recently, to further help reduce co2 emissions, the idea of using biological materials in vitrimers has been considered, as natural components are truly sustainable. To take a further step in this direction, the objective of this thesis is to study and characterize a vitrimer with methacrylate cellulose-based biological crosslinker, compared with a vitrimer with synthetic crosslinker, to evaluate any similarities or differences. Rheological and photoreological characteristics are studied by varying the percentages of biological crosslinker to define an ideal formulation printed by Digital Light Processing (DLP) photopolymerization technique. Extensive material analyses were conducted on this, including DSC, IR, swelling and gel percentage tests, combined with tensile tests to evaluate mechanical and self-healing characteristics after heat treatment. In the final stage of the work, considering the mechanical properties and the excellent printing fidelity measured, the possibility of using the analyzed material as a material for printing trabecular bone components was considered, with the aim of enabling simulations and mechanical test steps in the biomedical field, although further investigation needs to be carried out. This work opens the door to new studies and insights into the design of vitrimers with natural components.

CHAPTER 1: INTRODUCTION AND AIM OF THE WORK

In the biomedical industry, polymers are considered materials with enormous application potential due to their adjustable physico-chemical properties and interesting biological functionalities. Three categories of polymers are used depending on applications: thermoplastic polymers, hydrogels, and thermosetting polymers. The latter are often used because of their excellent mechanical and thermal properties, good fatigue and creep resistance, and ease and speed of production.

However, because of the irreversible chemical bonds created during the curing process, thermosets are inherently insoluble and infusible. Although these properties are regarded as major advantages during their life cycle, they become major limitations during the recycling phase. Most thermosets are disposed of in landfills or incinerated, and there are only a few alternatives for recycling, such as grinding and use as filler in other plastics, but this leads to the loss of value of the material, making it an unsustainable solution for the future (Figure 1). [1]

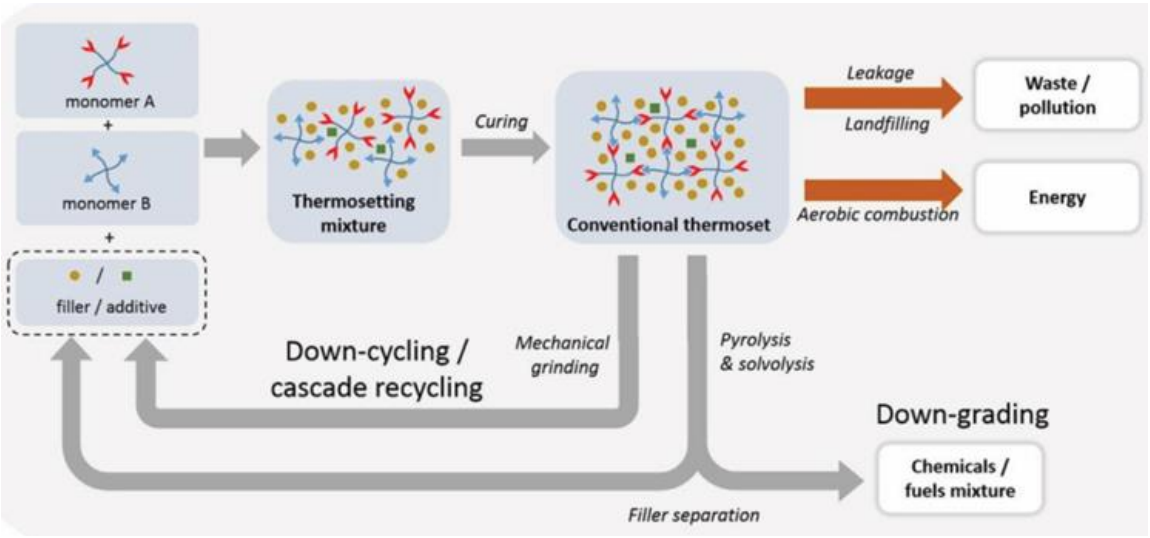

Figure 1: Overview of thermosets plastic material end-of-life employment [1]

In this context, this work aims to develop thermoset materials that maintain the same mechanical and thermal properties typical of irreversible bonds and the same ease of printing complex shapes, but in addition have sustainable features such as the ability to self-repair and the possibility of using biological materials for fabrication. These materials could be used in the biomedical field to reduce environmental impact.

Specifically, the proposed work aims to characterize a vitrimer with a cellulose-based biological crosslinker recovered from agricultural and industrial aloe vera and spirulina waste. This is compared with a vitrimer designed with the same monomeric components, but with a synthetic crosslinker, to assess any similarities and differences.

In the first phase of the project, the study investigated the rheological, photorheological, and stress-relaxation properties to evaluate the optimal methacrylate cellulose concentration. Once identified, the material was printed using Digital Light Processing (DLP) technology. Printing accuracy was evaluated using 3D scanners to compare the printed object with the CAD model.

Subsequently, in-depth analysis of the material was carried out, including DSC analysis of IR spectroscopy, swelling and recovery tests. In addition, tensile tests were conducted to evaluate the Young's modulus of the initial vitrimer and the vitrimer after heat treatment, which were useful to verify the self-repair and reprocessability properties.

Given the mechanical properties obtained and the excellent printing resolution, the possibility of using the studied vitrimer as a substitute for thermoset materials used in the fabrication of anatomical prostheses for testing was evaluated.

CHAPTER 2: CANS AND VITRIMERS

Polymeric materials can be classified considering different aspects, for example based on their origin, structure, crystallinity, or preparation technique. At the engineering level, a common classification is based on thermomechanical behavior, which distinguishes polymers into thermoplastics and thermosets.

Thermoplastic polymers are polymers formed by linear or loosely branched chains that are not cross-linked together. This structure generally gives these materials good deformability and reprocessability because it is sufficient to increase the temperature to bring them to a viscous state and be able to reprocess them. However, thermoplastics may have some limitations such as poor thermal stability at high temperatures and poor chemical resistance to some solvents. [2]

Thermosetting polymers instead consist of chains cross-linked to each other by irreversible covalent bonds. They exhibit excellent mechanical and thermal properties, excellent solvent resistance, and also are very easy and quick to manufacture, making them ideal materials for many biomedical applications. However, the inability to deform or reprocess these materials after cross-linking severely limits their ability to be recycled; in fact, methods for small-scale recycling which have been developed are not yet economically feasible, so quaternary recycling remains the most common technique (incineration). [2]

The concept of Polymer Networks with Adaptable Covalent Bonds (CANs) emerges in this context. CANs have dynamic covalent bonds that, under the action of external stimuli such as temperature, light, and pH, allow the reorganization of networks during the process. They represent a promising class of materials that are more sustainable and recyclable, capable of being reprocessed like thermoplastic polymers but exhibiting mechanical properties similar to thermosetting polymers.

CANs are generally divided into two groups depending on the exchange mechanism: associative CANs and dissociative CANs. In the first case, the covalent adaptable network employs associative bonds between polymer chains, where the original crosslink is only broken when a new covalent bond is formed in another position. In the second group, chemical bonds are first broken and then reformed in another position, causing a temporary net loss of crosslinking density (Figure 2). [3]

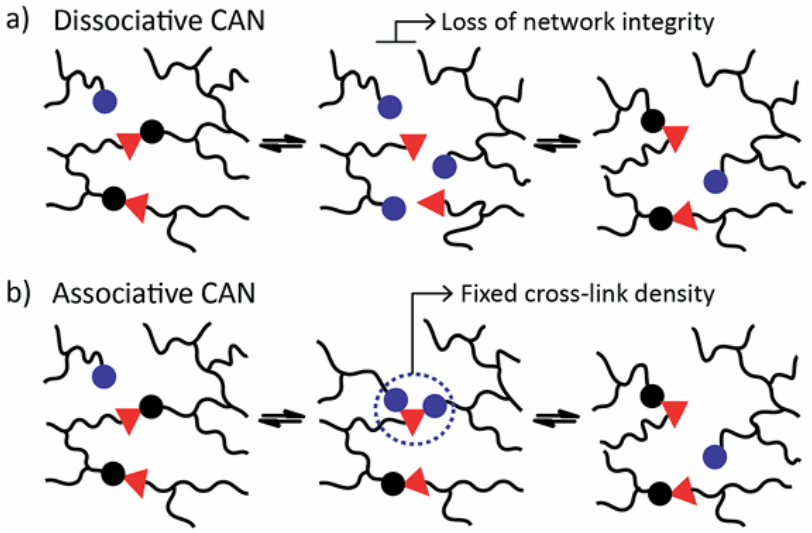

Figure 2: (a) dissociative CAN; (b) associative CAN [1].

In the past ten years, polymer materials based on associative CANs, known as vitrimers after the pioneering work of Leibler in 2011, have attracted strong interest in the scientific community. Vitrimers are polymers consisting of reversible networks capable of reorganizing their topology while keeping the number of chemical bonds and crosslinking density constant. Within a certain temperature range (depending on the polymer's characteristics), they behave like thermosetting polymers, therefore showing good mechanical characteristics at the service temperature. But when heated above a specific temperature, rapid dynamic exchange reactions occur allowing significant reorganization of the network without risk of structural damage (Figure 3).

Above the characteristic temperatures, vitrimers exhibit new properties such as healability, malleability, reprocessability, and recyclability, particularly interesting in terms of reducing environmental impact (more details will be given in paragraph 2.1.2).

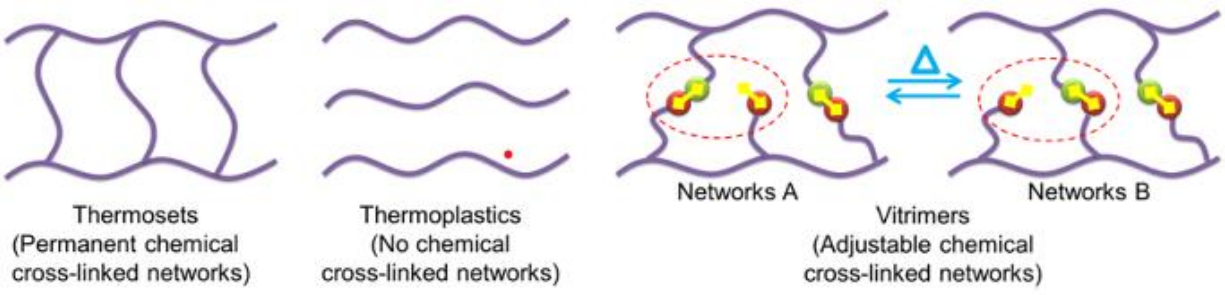

Figure 3: difference in molecular topology of thermosets, thermoplastics and vitrimers

2.1 VITRIMERS PROPERTIES

2.1.1 VISCOSITY BEHAVIOR

One of the characteristics that distinguishes vitrimers from dissociative CANs and thermoplastic materials is the viscosity behavior. At higher temperatures, the viscosity of vitrimers is essentially controlled by chemical exchange reactions, which lead to a decrease in thermal viscosity following the Arrhenius law:

$$\eta = \eta_0 \exp\left(\frac{E}{RT}\right)$$

Where $\eta 0$ is a pre-exponential factor, E is the activation energy, R is the universal gas constant, and T is the temperature.

The viscoelastic behavior of vitrimers can be described using two transition temperatures: the glass transition temperature (T_g) and the topology freezing temperature (T_v).

T_g indicates the temperature at which the polymer network changes from a glassy state to a rubbery state due to long-range molecular motion. T_v marks the transition from a viscoelastic solid to a viscoelastic liquid, conventionally chosen at the point where a viscosity of 10^{12} Pa·s is reached [4]. Since a reorganizing polymer network has a higher expansion coefficient than a static network, T_v can be experimentally observed through dilatometry.

These two transition temperatures can be controlled through parameters such as crosslinking density, intrinsic stiffness of monomers, kinetics of exchange reactions, and density of exchangeable bonds and groups.

There are two possible scenarios regarding the two above-described transition temperatures (Figure 4).

If the vitrimeric system has a T_g lower than the topology freezing temperature T_v, when it is surpassed, the solid behaves like an elastomer until, after overcoming T_v, it transforms into a viscoelastic liquid whose viscosity is controlled by the Arrhenius law [5]. An example of materials exhibiting this behavior was studied in the work of Bose, who developed a vitrimere by reaction between a castor oil-based dynamic crosslinker (iCO) and ABS PCR. This material has a glass transition temperature of 105°C and a topology freezing temperature of 183°C [6].

On the other hand, if the vitrimeric system has a T_g higher than T_v, no segmental movements occur. Overcoming T_g, segmental movement is gradually initiated, and it is observed that the kinetics of the rearrangement process are initially controlled by diffusion, following the William-Landel-Ferry (WLF) model, and subsequently by an Arrhenius-type behavior [5]. An example of vitrimeric

materials with these characteristics was described in the work of Dhers and coworkers, who developed a biobased vitrimer using a furan dialdehyde combined with a mixture of amines of biological origin. In their study, the glass transition temperature was measured at -10°C, while the topology freezing temperature was recorded at -60°C [7].

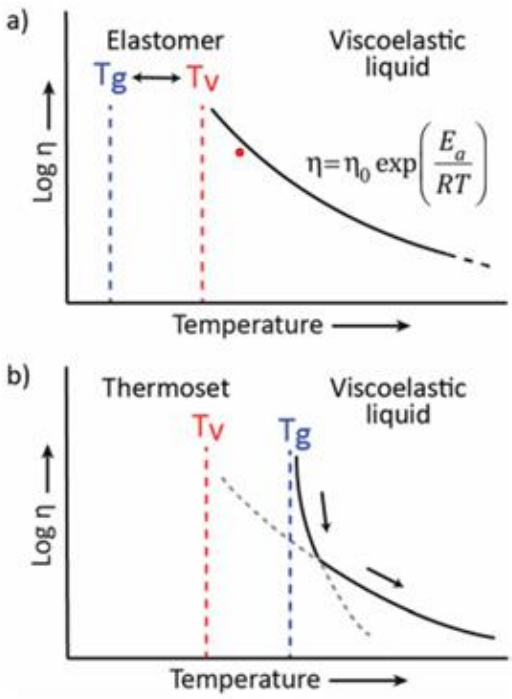

Figure 4: Viscoelastic behavior of vitrimers: a) Tg less than Tv; b) Tg higher than Tv [5].

The viscoelastic behavior of vitrimers is often demonstrated through stress relaxation experiments. In early studies on vitrimers, stress relaxation was modelled using a Maxwell equation:

$$\frac{G}{G_0} = e^{-\frac{t}{\tau*}}$$

where the relaxation time $\tau*$ is obtained when $\frac{G}{G_0} = \frac{1}{e} \approx 0{,}37$ (Figure 5). [1]

Several studies have highlighted that the Maxwell model is often unable to accurately model the data, as there are different relaxation modes based on the chemical conditions of the dynamic bonds present in the network. A more realistic model is obtained by adding a parameter β that reflects the relaxation distribution (with β = 1 resulting in the Maxwell model): [1]

$$\frac{G}{G_0} = e^{-(\frac{t}{\tau*})^{\beta}}$$

While a trend like the one described above is common in vitrimers, dependence on Arrhenius is not sufficient to determine if a system is actually a vitrimer, since dissociative CANs also show this

relationship. However, vitrimers are distinguished from dissociative CANs by having a constant crosslink density over a wide range of temperatures, which prevents vitrimers from dissolving in solvents and causes them to swell. The constant crosslink density can be verified through dynamic mechanical analysis or frequency sweep.[1]

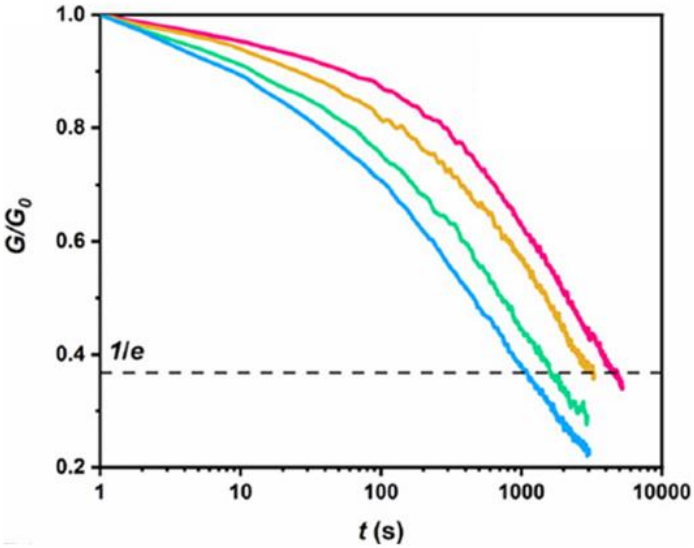

Figure 5: Vitrimeric trend evidenced by stress relaxation tests [3].

2.1.2 CHARACTERISTICS OF VITRIMERS

Thanks to the gradual decrease in viscosity with temperature, vitrimers can be easily reshaped by heating, and after heat treatment, additional properties are showcased.

One example is the self-healing capability that allows full or partial recovery of the material's mechanical properties, alleviating material waste problems due to replacing of damaged components and reducing the overall cost. Self-healing also enables welding processes of different and incompatible polymers and imparts adhesive properties: compared with traditional adhesives, vitrimer adhesives possess outstanding properties, including high transparency, strong adhesion, excellent mechanical properties and chemical resistance. [8]

Another aspect to consider is the shape memory property, which gives vitrimers programmable behavior, allowing them to change from two-dimensional to three-dimensional structures by external stimuli. [8]

In addition, vitrimeric materials have enormous recycling potential, making them particularly attractive from the perspective of reducing environmental impact. In most cases, vitrimers can be reprocessed by hot pressing the fragments into a new film. The reformed sample has a network architecture and mechanical behavior comparable to that of a fresh sample. in other cases, however, a chemical recycling system called depolymerization is possible, which allows monomer

recovery by immersion in reactive solvents (e.g., ethylene glycol for vitrimers based on transesterification) (figure 6).[8]

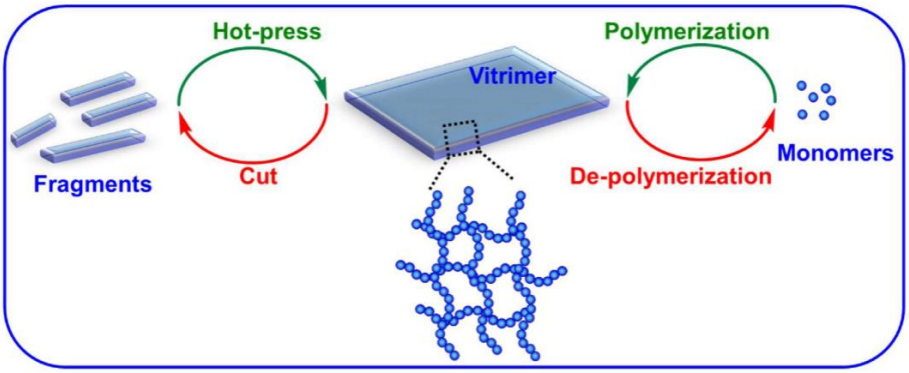

Figure 6: Schematic illustration of vitrimers recycling mechanisms [8]

2.2 DYNAMIC TRANSESTERIFICATION REACTIONS

Over time, vitrimers based on various dynamic exchange reactions have been studied and characterized, including transesterification, transamination, transcarbamoylation, disulfide exchange, imine exchange, and many others. Among these, transesterification mechanisms have been extensively studied as they are simple to synthesize and suitable for a wide range of monomers, making them perfect for industrial applications. Transesterification is a chemical reaction that involves the exchange of an ester with an alcohol in the presence of a catalyst (Figure 7). Thanks to the catalyst, it is possible to control the kinetics of the exchange reaction. By changing the type and amount of catalyst, it is possible to regulate the activation energy and the glass transition temperature without compromising the material properties. [3]

Transesterification also provides interesting characteristics to the material, such as flexibility, adhesion, and water resistance. One of the main problems with transesterification-based vitrimers is the long-term stability of the material; in fact, rapid processing requires high temperatures and high amounts of catalyst, and the solubility, aging, or washing of the catalyst could lead to instability, especially for materials with a high glass transition temperature (>75°C).[5]

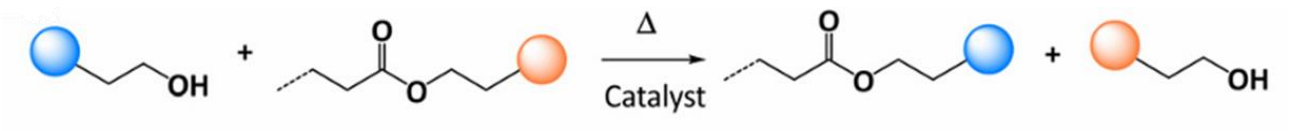

Figure 7: Transesterification reaction between an ester to an alcohol to obtain another ester and another alcohol[3]

2.3 BIOBASED VITRIMERS

The use of recyclable and biodegradable materials in vitrimers is a very promising idea, especially considering the pressure from environmental regulations and the importance of reducing CO2 emissions. Vitrimers based on biological substances can offer numerous advantages, such as the availability of biobased additives and their true sustainability, allowing for materials to be designed from the start to adapt to their future life cycle. These materials retain excellent mechanical properties and achieve high self-healing efficiency, allowing for reprocessing at temperatures where conventional polyester materials are processed. [9]

In the following section, some materials of biological origin, with aromatic and aliphatic chemical structure, commonly used in the preparation of vitrimers, will be analysed.

2.3.1 VITRIMERS FROM BIOBASED AROMATIC PRECURSORS

VITRIMERS FROM LIGNIN AND ITS DERIVATIVES

Lignin is a complex polymer mainly found in plants and in the cell walls of wood. It is formed in vivo through the enzymatic polymerization of various phenolic alcohols and has been widely used in thermosetting materials such as epoxy and phenol-formaldehyde resins.

Due to its aromatic structure and high molecular weight, lignin is often not compatible with other components, requiring chemical modification before use (Figure 8). [1]

An eco-friendly technique is ozonation, which involves breaking down the benzene rings of lignin and introducing carboxylic acid groups, improving the solubility of degraded lignin and allowing for easy removal. This technique was used in the work of Zhang and colleagues, where Kraft lignin was treated with ozone to prepare ozonized lignin (Oz-L) with abundant carboxylic acid and phenolic groups. The modified lignin was polymerized with an epoxy compound derived from sebacic acid in the presence of a zinc catalyst. Increasing the lignin content enhanced the Tg, modulus, and tensile strength of the prepared materials. Above 160°C, the studied materials showed rapid stress relaxation in the network and excellent shape memory, self-healing, and malleability properties.[10]

There are, however, other methods of modification besides ozonation. An example is the work of Hao and colleagues where chemically modified lignin with methyl hexahydro phthalic anhydride (MHHPA) was used to obtain a polycarboxylic acid derived from lignin (L COOH). This was used as a hardening agent to react with a PEG epoxy resin. The vitrimers obtained showed excellent self-healing properties and ease of removal, ideal for example for the design of coatings.[11]

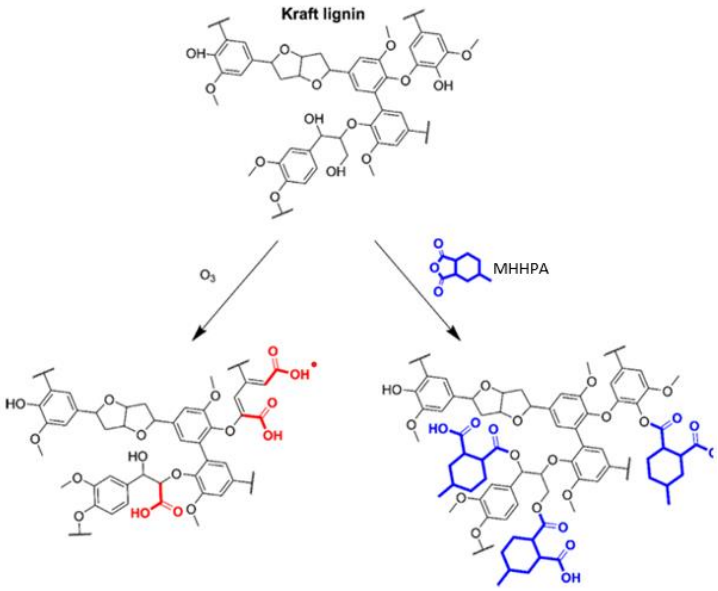

Figure 8: chemical modification of kraft lignin to introduce COOH groups [1]

In recent works, a derivative of lignin is often used: vanillin. In the study by Memon and colleagues, a new biobased epoxy hardener containing imines from vanillin and isophorone diamine (IPDA) was synthesized (Figure 9). The epoxy resins polymerized with these hardeners show high thermal performance, with a T_g exceeding 120°C, and excellent mechanical properties, including tensile strength and resistance to solvents and strong acids (pH=0). Furthermore, these resins are easily reprocessable through hot pressing without the use of catalysts or additives and can also be recycled in a closed-loop process. The tensile strength after recycling is very high, exceeding 70% after three reprocessing cycles. [12]

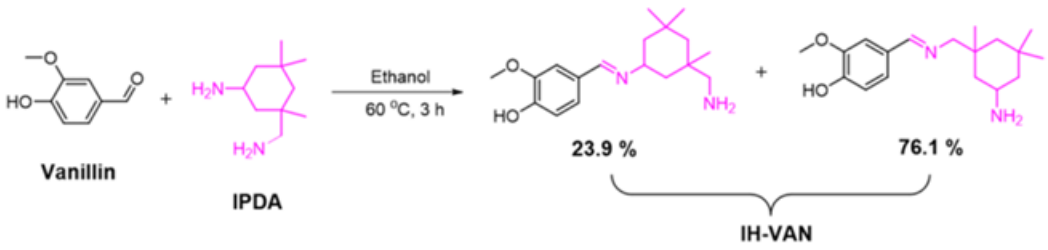

Figure 9: Synthesis of a vanillin-based vitrimer [12]

The need to modify lignin before use remains one of the most important limitations, as it requires the use of potentially hazardous chemicals during the material pretreatment, resulting in the production of toxic chemical waste. [9].

2.3.2 VITRIMERS FROM BIOBASED ALIPHATIC PRECURSORS

VITRIMERS FROM TRIGLYCERIDES AND FATTY ACIDS

Triglycerides can be obtained from various sources such as vegetable oils, microalgae and animal fats. They consist of glycerol and fatty acids with long hydrocarbon chains. The chemical structure of fatty acids, particularly the presence of unsaturated bonds, provides many opportunities for chemical modifications, making them one of the most commonly used biobased resources for polymer synthesis. Of these, vegetable oils are the most widely used as they are produced on a large scale and at a low price [1].

One example is soybean oil, composed mainly of oleic acid (one unsaturation) and linoleic acid (two unsaturations). Soybean oil can be epoxidized to produce ESO, a commercial product available on a large scale that shows great potential for the synthesis of vitrimers as a multifunctional epoxy resin. In a recent work by Wu and colleagues, a fully organic and recyclable vitrimer was developed from epoxidized soybean oil (ESO) and natural glycyrrhizic acid (GL) that has not been chemically modified to avoid the use of non-renewable petroleum resources and material disposal problems (Figure 10). Due to the rigid structure of GL, ESO/GL vitrimers have good thermal stability above 200°C and good mechanical properties. The transesterification reaction allows rearrangement of the polymer network leading to high welding performance, and excellent repair and shape memory characteristics. These materials are degradable to ethylene glycol, which makes chemical recycling easy. [13]

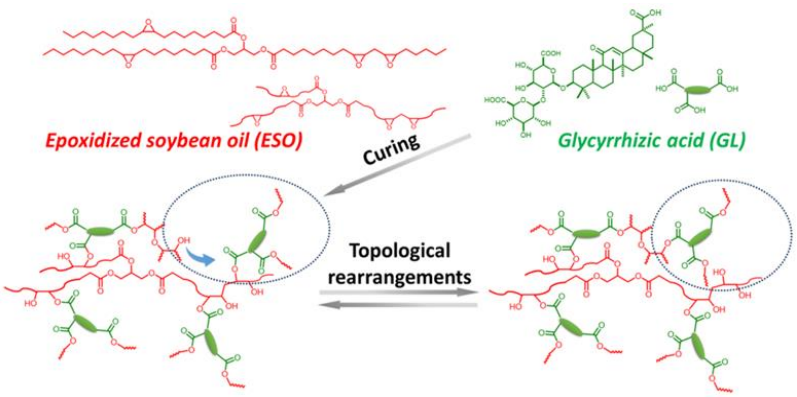

Figure 10: chemical structures of ESO and GL, curing reaction and rearrangements of network [13]

Another study developed a fully bio-based vitrimer using ESO and a rosin derivative fumaropimaric acid (FPA), in the presence of catalyst (Figure 11). Again, the vitrimer demonstrates excellent self-healing, shape memory and high tensile strength due to the rigid structure and tricarboxylic groups

of FPA. Dynamic transesterification exchange reactions allow degradation of the ESO-FPA material in pressure reactor at 140 °C and reprocessing into new vitrimers at 180 °C [14].

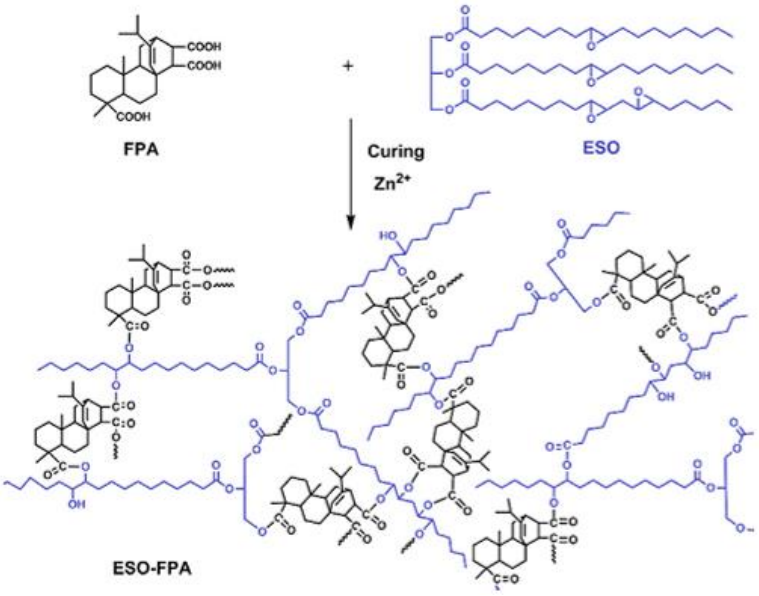

Figure 11: chemical structures of ESO and FPA, curing reaction [14]

A significant obstacle in the synthesis of vegetable oil-based vitrimers is the production of materials with good strength characteristics and high glass transition temperatures.

VITRIMERS FROM CELLULOSE

Cellulose is the most abundant biopolymer on Earth and is mainly contained in plants. It consists of glucose molecules linked by a glycosidic bond, forming an unbranched polymer chain.

Several studies have reported the use of cellulose derivatives such as cellulose paper, nanocrystals, and carboxymethyl cellulose for the synthesis of vitrimers because the functional groups of cellulose derivatives (OH, COOH, or carboxymethyl) are ideal for transesterification and transcarbonation reactions.

In a study by Zhao and colleagues, cellulose paper was used as reinforcement. A vitrimer was made for the first time using polycarbonate as the matrix and natural cellulose paper as the reinforcement structure, catalyzed by Ti(IV) for transcarbonation. Polymerization of the vitrimer was then conducted directly on the paper and involved the OH groups of cellulose (Figure 12).

The resulting materials have exceptional mechanical properties and great thermal/chemical stability up to 400°C. In addition, shape memory, self-repairing and recyclability characteristics of both polycarbonate and natural cellulose,under mild conditions, are shown. [15]

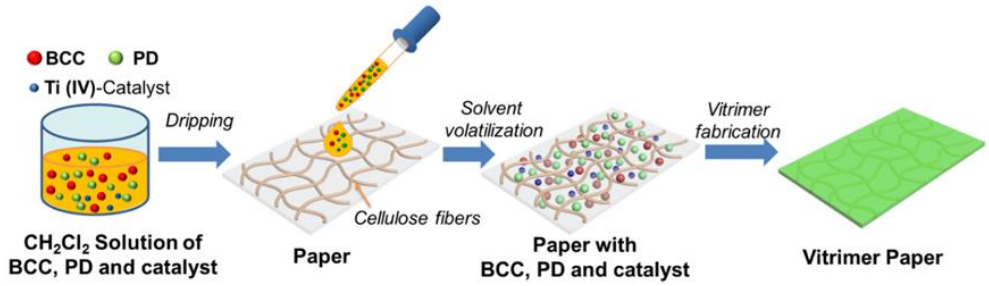

Figure 12: Schematic diagram of the fabrication of paper-reinforced polycarbonate vitrimer [15]

In another work, the possibility of using carboxymethyl cellulose (CMC) was investigated. CMC was polymerized with diglycidyl ether of bisphenol A (DGEBA) and glycerol, with catalyst added to promote transesterification, resulting in a stable polymer matrix. The obtained vitrimer has good thermal stability, mechanical strength and shape memory properties. In addition, thanks to the glycerol, there is great mobility, which is useful for promoting associative exchange and thus reprocessability of the material (Figure 13).[16]

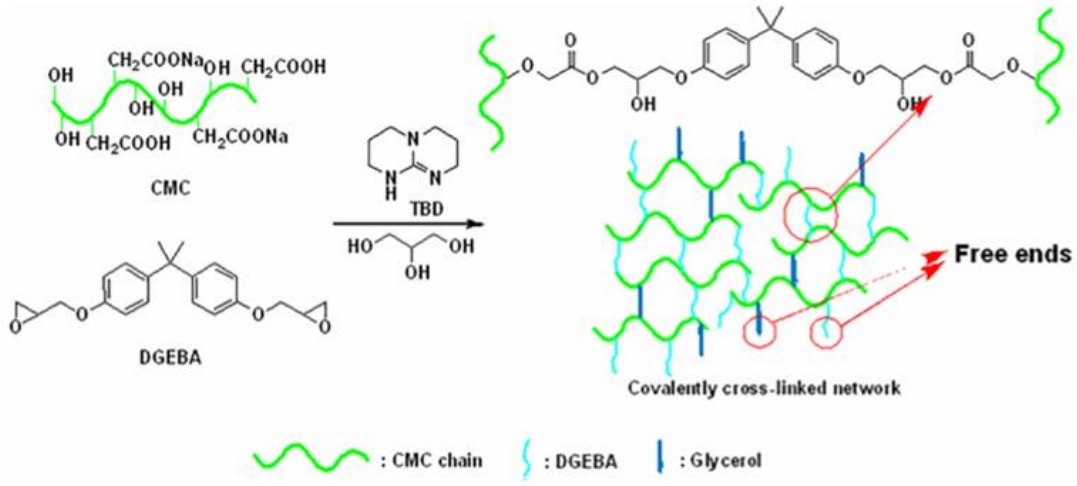

Figure 13: illustration of the CMC crosslinked DGEBA network based on epoxy-acid reaction [16]

In a recent work by Capannelli and colleagues instead, cellulose was used to improve the rheological behavior of the material. A vitrimeric material based on an epoxy-functionalized cardanol polymerized with a biobased polycarboxylic acid was developed. This soft polyester has been shown to be reprocessable and recyclable, but not suitable for 3D printing. Therefore, to improve the rheological behavior, cellulose powder was added as a modifier, which made the print more stable. Preliminary printing tests were positive, and the printed parts were subsequently thermally cured, leading to a vitrimer with excellent mechanical properties.[17]

2.4 BIOMEDICAL APPLICATION

As seen in Chapter 2.1.2, vitrimeric materials have attractive characteristics such as self-healing, shape memory, and the possibility of reprocessing and recyclability that make these materials suitable for real-world industrial applications. Vitrimers currently represent an alternative to conventional materials currently used in three macro areas: self-healing and reusable adhesives, shape memory devices, and three-dimensional printing applications[18].

In recent years, however, the properties of vitrimers have also attracted interest in the biomedical field, and some studies have been done to optimize vitrimeric compounds for biomedical applications.

One example may be the work of Xia and colleagues who designed a thermogelling vitrimer that, due to the addition of a blocking molecule, remains fluid at low temperatures and transforms into a thermally stable gel as temperature increases, creating a thermal equilibrium gel. This results in a covalently cross-linked vitrimers that can be reversibly modulated by varying the use of catalysts or the concentration of the blocking molecule. The adjustable mechanical properties and biocompatibility make this material promising for future biomedical applications, such as in tissue repair and non-invasive injectable surgical implants based on biocompatible silyl ether metathesis [19].

In addition, since vitrimers are materials with excellent printing resolutions they can be used in the future in combination with 3d anatomical modeling software, such as Hyper Accuracy 3D software (HA3D), for simulation and testing of anatomical prostheses.

With the ability to create detailed models and consequently simulate the procedure prior to surgery, surgeons can increase the efficiency and accuracy of procedures while reducing post-operative risks and complications. Particularly in orthopedic surgery, this approach gives the ability to accurately assess correlations between implants and patient anatomy, size prosthetic implant, analyze the amount of residual bone and deformities between bone segments, define resection margins for cancer cases and simulate fracture reduction and synthesis.

This innovative approach not only improves the quality of care provided to patients, but also allows for greater personalization of treatments, ensuring a surgical outcome tailored to each individual.

In addition, the ability to engage patients in understanding their clinical problems and decision making through visualization and simulation of their surgery contributes to greater awareness and a better overall patient experience. https://www.medics3d.com/en/

CHAPTER 3: 3D PRINTING

The process of 3D printing, also known as additive manufacturing ((AM) or rapid prototyping, involves creating three-dimensional objects by depositing layer after layer of a material. The necessary geometric information is contained in an STL file generated by CAD software, which subdivides the 3D object into individual layers that are then deposited in the X-Y plane and repeated along the Z axis until the desired object is fully realized. [20]

The main advantages of these techniques are the ability to produce complex geometries while maintaining good resolution, quickly and inexpensively without the addition of additional tools (e.g., molds). In addition, being a bottom-up process allows for less material waste.

It is because of these attractive features that 3d printing is widely used in many areas of industry including biomedical. It is possible to make customized implants for the patient, to create scaffold for tissue regeneration or to enable better communication between doctors and patients [21]

However, despite the potential of additive manufacturing technology, there are some shortcomings that limit its use, especially in mass production. Indeed, it is currently only possible to print small objects, and surface imperfections are often created due to the substrate material or overlapping powder particles. In addition, especially in the biomedical field there is limited availability of high-quality materials that meet the criteria established for medical applications. [22]

3D printing techniques can be divided into three macro categories:[20]

- Extrusion-based methods: thermoplastic filaments are melted by a heated nozzle to be deposited at the desired location, where they subsequently cool, solidifying in a short time. A common example is fused filament fabrication (FFF).
- Powder-based methods: a layer of fine powders is compressed and melted by a binder or laser irradiation to create the object. Selective laser sintering (SLS) falls into this category.
- Photopolymerization-based methods: monomers and oligomers are exposed to UV light that allows a photopolymerization reaction, leading the resin to solidify. The stereolithography technique called Digital Light Processing (DLP) falls into this category and will be discussed extensively in later chapters because it was used for this work.

3.1 PHOTOPOLYMERIZATION-BASED TECHNIQUES

Photopolymerization, often called vat-photopolymerization because of the container used in the process, is a 3D printing technique that enables the production of highly cross-linked polymer networks by exposing photosensitive monomers and oligomers to high-intensity light radiation (Figure 14), usually in the UV-visible light spectrum (250-450nm). [20]

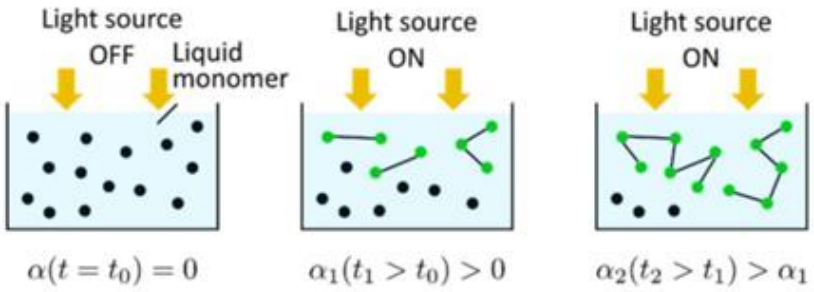

Figure 14: General photopolymerization scheme

The layers of the liquid precursor are exposed to light radiation one at a time and selectively allowed to solidify. After the development of a layer, the printing platform moves vertically, and a new liquid film is available for polymerization and subjected to the same process until it is complete.

The resin used as a precursor consists of a monomeric part, which will form the polymer network, and a photoinitiator that serves to convert light radiation into chemical energy. This process creates free radicals or cations that react rapidly with the monomers, generating the final material. In this process, it is essential that the photoinitiator has an absorption spectrum superimposed on the emission spectrum of the light source.

Light-curing resins can be divided into two categories depending on the polymerization mechanism they use [23]:

- Free-radical polymerization, where the reactive species that induces propagation is a free radical. This mechanism can be divided into three stages: initiation, propagation and termination. During the first stage, the light activates the photoinitiator and a radical is generated as a result. During propagation, the photoproduced radicals bind to monomers and monomeric radicals are generated that react with other monomers, creating a chain reaction. In the last step, the end of the reaction takes place. This can occur directly when two growing chains meet and the radicals neutralize each other, or, in the presence of impurities that block the active groups, by a process called disproportionation. A major problem with this mechanism is the oxygen inhibition of the radical groups, which changes

the kinetics of polymerization, slowing it down. A typical example of free-radical polymerization occurs in acrylates.

- Cationic polymerization where the reactive species is an ion, usually a cation. This mechanism is less common because it is slower and sometimes requires additional heat treatment to increase monomer conversion. In addition, the terminal phase does not occur directly, but by disproportionation in the presence of impurities or added reagents. Nevertheless, it is beginning to attract interest because epoxides, lactones and vinyl ethers, typical examples where cationic polymerization takes place, are insensitive to oxygen.

So-called hybrid systems, which involve mixing monomers that polymerize by different mechanisms, also exist in the literature. The use of such hybrid systems offers the possibility of producing interpenetrating polymer networks within seconds of UV irradiation. Moreover, with proper selection of the two components, the final properties of the polymerized polymer can be precisely controlled.[23]

There is a further classification based on the irradiation method used. Specifically, there are 3 different techniques: stereolithography (SLA), two-photon polymerization (TPP), and mask projection polymerization (figure 15). SLA uses a layer-by-layer vector scanning approach to create structures, where the laser beam travels according to a programmed path, curing the resin it comes in contact with. It is considered a relatively slow method of printing. In the TPP process, the laser is focused by a lens on a precise spot in the resin. The presence of photoinitiating molecules initiates the polymerization process, generating localized radicals through the absorption of two photons at the center of the focused beam, resulting in the formation of a volume pixel (voxel). Image projection techniques are very fast because they expose an entire layer of resin to the radiation at a time, masking the areas that are not to polymerize. They can be further classified as liquid crystal display (LCD) and digital light process (DPL), which will be described extensively in Section 3.1.1 as it is used for this work. [24]

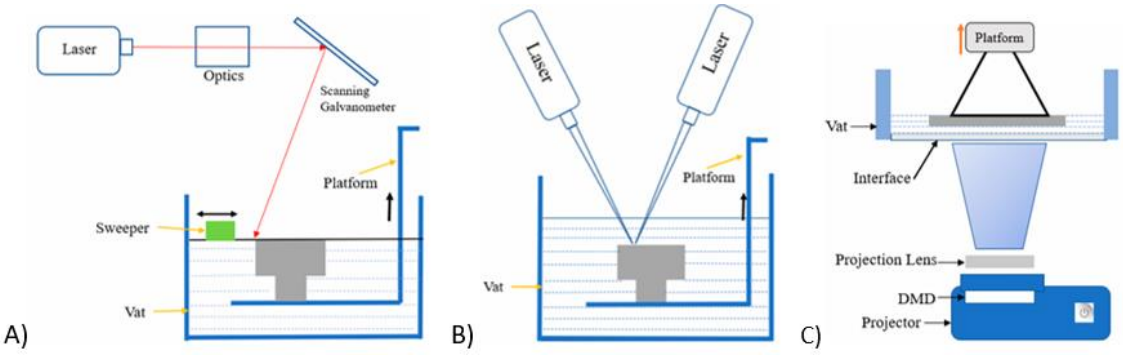

Figure 15: (a) SLA. (b) TPP. (c) DLP.[24]

All the previously described techniques fall under the Vat Polymerization (VP) technique, which is considered the most advantageous technique for 3D printing due to some specific features. For example, it has a high resolution, with a characteristic size usually lower than 50 µm and up to 100 nm for TPP, and the ability to change the final properties of the object due to changes in the chemistry of the initial resin [20]. In addition, unlike other 3D printing techniques, it does not require specific resin requirements such as surface tension, viscosity or volatility, but neither do support materials for particularly complex objects. In addition, it is possible to light-cure at room temperature and one can control the temperature rise during the reaction by changing the intensity and wavelength of irradiation. [23]

However, there are also some disadvantages. In fact, only one material can be used at a time during polymerization, and possible volume shrinkage at the end of the process must be considered. In addition, it is important to check the degree of polymerization achieved and possibly add an additional polymerization step, since unreacted material affects the final mechanical properties.[23] In the biomedical field, it is then of paramount importance to consider well the materials used because UV radiation can lead to degradation of the reactants and damage the inserted cellular components [25].

3.1.1 DPL: MECHANISM AND CHARACTERISTICS

Digital Light Processing (DLP) is a projection technology that uses microscopic chips to reflect light and create high-definition images. It is a constrained surface approach, with the light source placed under a transparent reservoir and the printing platform suspended above the resin bath.

Unlike other photopolymerization techniques such as SLA, in the DLP technique an entire layer of resin is irradiated at once, and by inserting a digital micro-mirror device (DMD) into the optical path of the laser, the UV light can be modulated and thus polymerize each individual layer with the desired shape (Figure 16). [26]

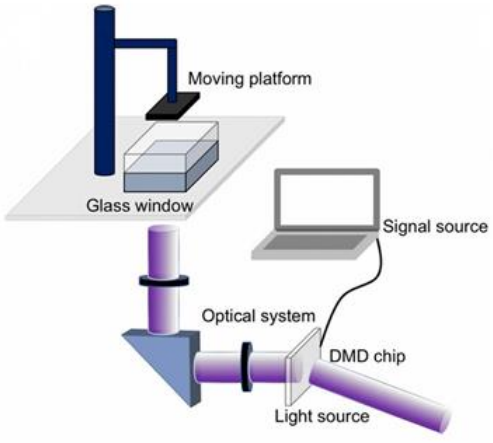

Figure 16: Schematic of the DLP-based 3D printer [27]

Specifically, the DMD is the key component and serves as a dynamic mask for the process. It consists of a series of movable micro-mirrors that can be individually set to an "on" or "off" state. Each mirror represents a single pixel, and the individual tilt of each mirror enables fast and reliable pixel switching. The high switching speed of the DMD is a prerequisite for realizing grayscale illumination, which can be useful for precise control of exposure time and energy dosage per measurement. [26] Once the printing process is completed, the printed object must be removed from the platform and appropriate solvents must be used to remove excess resin. Usually, the object undergoes a post-polymerization treatment in a UV chamber to complete the conversion and achieve better mechanical properties.

The DLP technique is widely used because it has some very interesting advantages. For example, it can achieve resolutions on the order of 25 µm, but are reported studies in which sizes even smaller than 0.6 µm have been reach [28]. The technique is also very fast, due to the irradiation of the entire working layer, and economical since a reduced amount of resin is needed because the sample does not need to be completely submerged in the reservoir. DLP technology is also a so-called "free-form" technology in that no support structure is needed even for particularly complex geometries such as hollow or porous components. Because of all these features, it is widely used in some biomedical areas such as tissue engineering, drug delivery, or implantation. Currently, many have built tissue structures such as bones, blood vessels, nerves, spinal cord, cartilage, and trachea through DLP printing technology although the optical transparency of bio-inks and the difference in the growth rate of cellulases between different areas of the printed object remain major limitations to be investigated.[27]

However, this technique has some disadvantages. The main one is related to the adhesion between the parts and the bottom of the vat, which must be overcome for the newly solidified layer to adhere

to the previous layers. Several methodologies are used to reduce the intensity of these forces, including the application of hydrophobic coatings to the bottom of the tank. In addition, the pixel-based exposure mechanism can cause sawtooth surface roughness on curved surfaces. Consequently, when aiming for higher resolution, the pixel size must be reduced with the help of designated optics. Since the DMD has a fixed number of mirrors, this leads to image shrinkage and reduces the maximum size of the geometry. Large parts are therefore often printed at lower resolutions than small parts.

Another important aspect to consider is that during DLP printing, the extra energy of UV light can cause over-curing of the light-curable material, reducing the printing resolution and interfering with curing of the next layer. To avoid this problem, it is necessary to dissipate the extra energy of the UV light by holding the printed structure in the air for a period of time, which inevitably increases the printing time. To solve this, however, the concept of continuous DLP printing has been implemented in recent years. Tumbleston and colleagues developed the CLIP (Continuous Liquid Interface Production) method by applying an oxygen-permeable window below the ultraviolet image projection plane. This window creates a persistent liquid interface called a "dead zone" to achieve continuous printing and thus improve print fidelity and reduce total time.[26]

3.2 3D PRINTING FORMULATIONS

In the context of 3D printing, the main elements present in a photocurable resin are the photoreactive precursors, such as monomers and oligomers, together with at least one photoinitiator, which can be of the radical or cationic type. These are responsible for the chemical reaction that leads to polymerization of the material. However, in addition to these essential elements, the resin formulation may also include various additives or fillers that can impart new properties to the printed material.[25]

PRECURSORS

Precursors are monomers, oligomers or prepolymers that solidify after exposure to light. The selection criteria are based on the application and technology to be used, and the principal aspects to be considered are the type of functionality (mono-, di-, or poly-), viscosity, reaction kinetics, hydrophobicity/hydrophilicity, shrinkage, cost, durability, volatility, and toxicity. The kinetics are mainly controlled by the reactive groups, while the core group mainly influences the physicochemical and mechanical properties of the final polymer.[29]

Some of the most used resins are composed of acrylate precursors, which act by radical polymerization mechanism. The preference for acrylates is due to their high reactivity during polymerization and their ability to promote adhesion between print layers. However, during the curing process, acrylates can contract, causing problems with poor resolution, internal stress or deformation and printing defects. To reduce these negative effects, high-molecular-weight oligomeric acrylates can be used, but they have limited mobility and viscosity (diluent is needed) and are sensitive to the presence of oxygen, which can interfere with the curing process.

Some of the most common precursors used in 3D printing are polyethylene glycol diacrylate (PEGDA), triethylene glycol dimethacrylate (TEGDMA), bisphenol A-glycidyl methacrylate (Bis-GMA). [25]

For more specific applications, however, resins based on thio-ene/-yne and epoxy systems are used, which are known for reduced shrinkage, lower stress and higher conversion than acrylates. The C-S-C bonds in thio-ene may exhibit low mechanical properties, but these can be improved by adding allyl ethers to the blends. In addition, thio-ene networks offer a high reaction rate and lower sensitivity to oxygen inhibition than other mechanisms. [29]

Common thiol monomers suitable for the 3D printing are trimethylolpropane tris(3-mercaptopropionate)(TMPMP) and pentaerythritol tetra(3-mercaptopropionate)(PETMP) [25].

Resins based on epoxy systems, on the other hand, cure through a cationic mechanism. Cationic photopolymerization is slower than radical polymerization, but this allows lower residual stresses that improve the mechanical properties of the components. Conversely, this type of photopolymerization can be inhibited by high ambient humidity.

Mixtures of various types of acrylic and epoxy precursors are often used to get the best possible properties.

PHOTOINITIATORS

A photoinitiator (PI) is the component that creates reactive species (free radicals, cations or anions) when exposed to light radiation and thus allows the polymerization reaction to be initiated. It is crucial that the absorption/reactivity window of the photoinitiator matches the wavelength used by the 3D printer.

In general, photoinitiators are divided into two types: type I photoinitiators, such as dimetilpiridinil ossido (DMPA) and 2,4,6-trimetilbenzoil-fenilfosfinico (TPO), which undergo fragmentation to form radicals upon irradiation, and type II photoinitiators, such as riboflavin and triethanolamine, which

require co-initiators and undergo hydrogen atom abstraction to form radicals. The type of photoinitiator and its amount significantly influence the reaction kinetics, conversion and mechanical properties of the final object, so it is important to evaluate its choice well. [30]

ADDITIVES

Additives are not necessary, but they can be added to improve the quality of the resin and the printing process. Some examples of additives may be [29]:

- Dyes: they absorb incident UV and visible light and thus serve to improve printability and print resolution, although some dyes are used only for aesthetic purposes. Choosing the correct dye depends on the absorption spectrum of the photoinitiator and the wavelength of the printer. They are usually dispersed in the liquid formulation, but some can be covalently bound to the polymer. An example of a widely used dye is Sudan I, which is used to control the depth of cure and improve Z resolution.
- Absorbers: are used to absorb the light beam and thus decrease the depth of light penetration, to avoid over-polymerization in the vertical direction and improve resolution. The most used UV absorbers are benzotriazole derivatives.
- Thinners: are used to reduce the viscosity of the resin when too high temperatures cannot be used to reduce it.
- Rheological additives and stabilizers: these are used to prolong the life of the resin and its stability during longer prints.

FILLERS

Fillers serve to overcome the limitations of polymeric materials by imparting specific properties such as electrical and thermal conductivity, luminescence, stiffness, electromagnetic shielding and antibacterial properties. They also allow for improved printing accuracy as they reduce material shrinkage. It is important to verify that the addition of fillers does not compromise the stability of the resin during printing, to avoid agglomeration or settling. The most frequently used fillers are carbon materials (e.g., graphene and nanotubes), ceramic and metal powders, glass and fibrous materials [42] (e.g., such as cellulose), minerals (e.g., such as titanium), and bio-fillers (e.g., such as coffee grounds and wood flour) [29].

CAPITOLO 4: MATERIALS AND METHODS

4.1 MATERIALS FOR 3D PRINTING

All materials used in this thesis work were purchased from Sigma-Aldrich (Merck Company, Milan, Italy), except for methacrylate cellulose which was synthesized in collaboration with Università degli Studi di Cagliari, Complesso Universitario di Monserrato (Cagliari, Italy).

FUNCTIONAL MONOMER

For this work, 2-Hydroxy-3-phenoxypropyl acrylate (HPPA) was used as a functional monomer. This is indicated in the synthesis of vitrimers because it has hydroxyl and ester groups used in the transesterification reaction. In addition, the presence of the benzene ring can enhance the thermal and mechanical properties of the final polymer.[31]

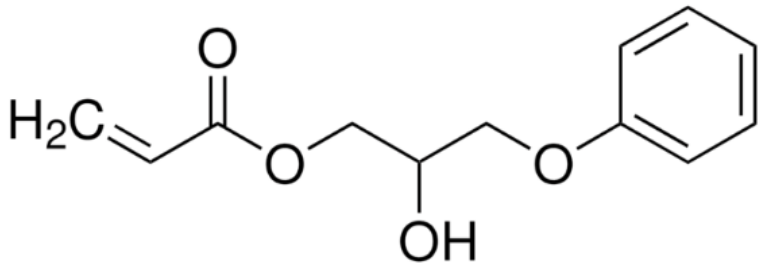

Figure 17: chemical structure of 2-hydroxy-3-phenoxypropyl acrylate (HPPA) [32]

CROSSLINKER

Glycerol 1,3-diglycerolate diacrylate (GDGDA) was used in the formulation of the synthetic vitrimer. It is a polyol ester with a molecular structure comprising three fatty acids, two of which are acrylate-based, linked to a glycerol skeleton. GDGDA is used as a crosslinker because when exposed to ultraviolet light or other suitable light sources, it induces crosslinking and curing processes. It also serves to have a high number of -OH groups in the polymer network, which are useful for transesterification. [33]

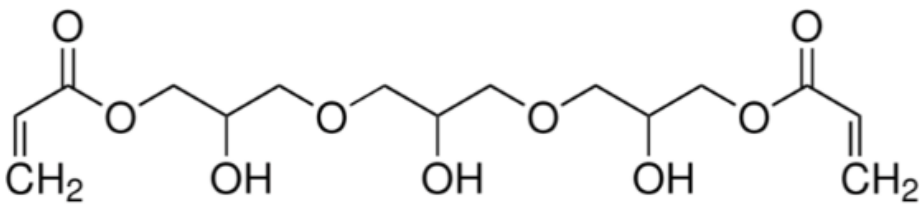

Figure 18: chemical structure of Glycerol 1,3-diglycerolate diacrylate (GDGDA)[34]

Methacrylate microcrystalline cellulose (MCC) was used in the formulation of natural vitrimer. This substance is synthesized from partially depolymerized cellulose by treatments with mineral acids

and then hydrochloric acid. MCC is rich in hydroxyl (OH) groups, allowing this material to be used as an excellent crosslinker in transesterification reactions.[35]

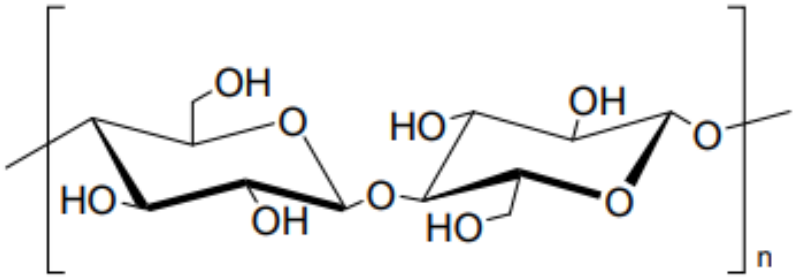

Figure 19: chemical structure of Methacrylate microcrystalline cellulose (MCC) [35]

CATALYST

Miramer A99 was used as catalyst. This is a methacrylate phosphate compound that acts as a transesterification catalyst at high temperatures and as a stabilizer for the other components. [36]

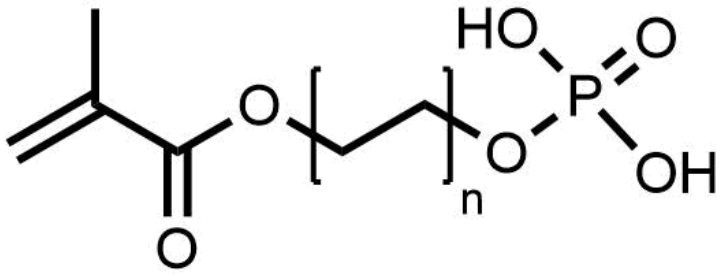

Figure 20: chemical structure of Miramer A99 [33]

PHOTOINITIATOR

Phenylbis (2,4,6-trimethylbenzoyl) phosphine oxide (BAPO) was chosen as the photoinitiator because it adequately absorbs the emission wavelength of the 3D printer used (385 nm).

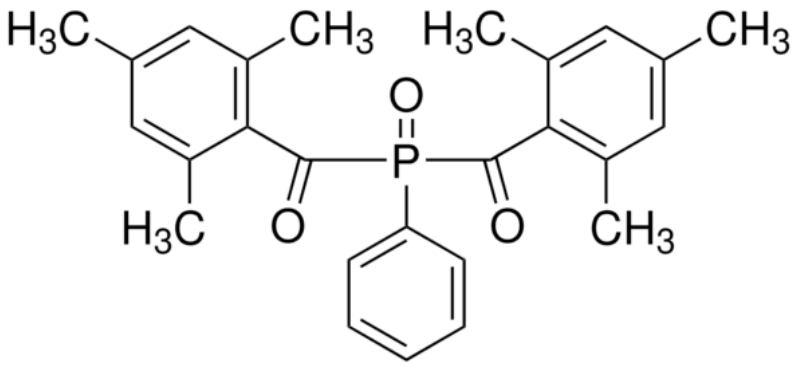

Figure 21: chemical structure of Phenylbis (2,4,6-trimethylbenzoyl) phosphine oxide (BAPO)[37]

4.2 PREPARATION OF 3D PRINTING FORMULATION AND PRINTING PROCEDURE

4.2.1. SYNTHESIS OF METHACRYLATE CELLULOSE

Cellulose, dimethylformamide (DMF) and methacrylate anhydride with respective weight ratios of 20:40:40 were used for the formulation.

Once the formulation was made homogeneous, it was left overnight at 70°C under a fume hood. Then the acrylate cellulose was washed three times in EtOH, filtered on a buchner filter and allowed to dry at 40°C overnight in vacuum. [38]

The cellulose used in this work is derived from agro-food waste of aloe vera (VIVA3D project supported by MASE).

4.2.2 FORMULATION'S PREPARATION

Four light-curable formulations were prepared with different weight ratios between the functional monomer (HPPA) and the crosslinker, while the weight of the catalyst (Miramer A99) was not changed:

1) HPPA : GDGDA : Miramer A99 = 75:10:15
2) HPPA : MCC : Miramer A99 = 80:5:15
3) HPPA : MCC : Miramer A99 = 75:10:15
4) HPPA : MCC : Miramer A99 = 70:15:15

In each formulation, 2 phr of BAPO photoinitiator was then added.

In formulation 1, a synthetic crosslinker (GDGDA) was used, and the vitrimers will henceforth be called "HG10" and used as the synthetic comparison vitrimers.

In formulations 2,3, and 4, a natural crosslinker (MCC) was used, and the resulting vitrimers will henceforth be called "HC5," "HC10," and "HC15," respectively.

In the first step, it is necessary to prepare a batch with functional monomer, crosslinker (GDGDA or MCC depending on the formulation) and catalyst together that are mixed by magnetic stirring at a speed of about 500 rpm to make the resin homogeneous. This step is especially important in formulations with natural crosslinker, as MCC tends to create lumps.

Next, BAPO is added and the final mixture is mixed again with magnetic stirrer until a perfectly homogeneous resin is obtained.

Each solution is prepared in a black falcon to avoid premature photopolymerization of the resin due to visible light.

4.2.3 PRINTING PROCEDURE

The Asiga MAX UVX27 printer, made by the company Asiga, was utilized for the printing stage (Figure 22). The LED light source used in this DLP printer emits light with a wavelength of 385 nm; on the x-y plane, pixels have a resolution of 27 µm, while along the z plane, it is between 1 and 500 µm. The construction platform has a surface area of 51.8 x 29.2 mm2, and the tallest object that may be printed is 75 mm high.

Figure 22: Asiga MAX UVX27 printer [39]

Layer thickness, light intensity, irradiation time and temperature of the printing environment are the main factors that can be changed from the default values set by the Asiga Composer software. The first three layers called "burn in" layers are printed with longer irradiation times than the subsequent layers to promote adhesion of the material to the platform. Table 1 shows the printing parameters used in all formulations.

Table 1: printing parameters

HG10, HC5, HC10, HC15		
	Burn-In	Other layers
Temperature (°C)	30	30
Slice thickness (mm)	0.07	0.1
Light intensity (mW/cm^2)	35	35
Exposure time (s)	2	1

After printing, the object is peeled off the printing plate with the help of a blade. It is then washed with acetone to remove residual resin.

Finally, the object is post-cured for 3 minutes per side using a Broad-band UV chamber from Asiga (light intensisty 10 mW/cm^2).

4.2.4 HEAT TREATMENT

For some tests that will be discussed in the next section, heat treatment of the printed material was required. The selected formulations were subjected to a 24-hour heat treatment in a MEMMERT BIOMed_vacuum oven at a controlled temperature of 180°C.

4.3 CHARACTERIZATION METHODS

In this section will be analysed the characterization methods used during the experiments. The materials analysed for each method of analysis are summarized in Table 2.

Table 2: Summary of characterization methods and formulation used

Analysis	Material analysed	Material type	Method of realization
Photorheology	HG10, HC5, HC10, HC15	liquid resin	-
Rheology	HG10, HC5, HC10, HC15	liquid resin	-
Stress relaxation	HG10, HC10	specimen solid	DLP + post-curing
Swelling test	HG10, HC10	specimen solid	DLP + post-curing
	HC10 TT	specimen solid	DLP + heat treatment
Recovery test	HG10, HC10	specimen solid	DLP + post-curing
	HC10 TT	specimen solid	DLP + heat treatment
DSC	HPPA, HC10 without MCC, HC10 without cat, HC10	specimen solid	DLP + post-curing
FTIR-ATR spectroscopy	HC10	liquid resin	-
	MCC, HPPA, HC10 without MCC, HC10 without cat, HC10	specimen solid	DLP + post-curing
	HC10 TT	specimen solid	DLP + heat treatment
Mechanical characterization	HC10	specimen solid	DLP + post-curing
	HC10 TT	specimen solid	DLP + heat treatment
3D scanner	HC10	specimen solid	DLP + post-curing

4.3.1 RHEOLOGY AND PHOTORHEOLOGY

PHOTORHEOLOGY

A photorheology test was conducted to study the polymerization kinetics of formulations in response to light irradiation.

The test used is called the oscillatory sweep and consists of evaluating the time course of the conservative modulus (G') and the dissipative modulus (G"), keeping frequency and amplitude of oscillation constant. G' and G" are quantities that describe the viscoelastic behavior of the polymeric material: when the material is liquid, the viscous modulus is higher than the elastic modulus (G">G'); when the material is solid, such as a result of cross-linking, the elastic modulus becomes higher (G'>G").

During the test, if the material cross-links, a reversal point should be observed where the elastic modulus curve exceeds the viscous modulus curve. This point is called gel point and is particularly important in 3D printing processes because it must be exceeded to allow the layer to solidify.

The oscillatory sweep test is divided into 3 stages:

1) Starting the test and monitoring G' and G"
2) Turning on the UV light to start the crosslinking of the resin
3) Monitoring of G' and G" until the plateau is reached.

From the curves obtained, it is important to consider the time delay separating the lamp ignition from the gel point and the slope of the growth stretch of the two modules to assess the rate of reaction propagation.

In this thesis, a Hamamatsu LC8 broad-spectrum UV lamp and an Anton Paar MCR 302 rheometer with a coupled flat-plate type configuration were used to perform the test, as schematized in Figure 23. A glass plate transparent to the incident UV beam was used for the bottom plate of the rheometer (to avoid ruining the quartz plate, usually used for this test, with highly reactive and adhesive resins). The parameters used for all formulations are given in Table 3.

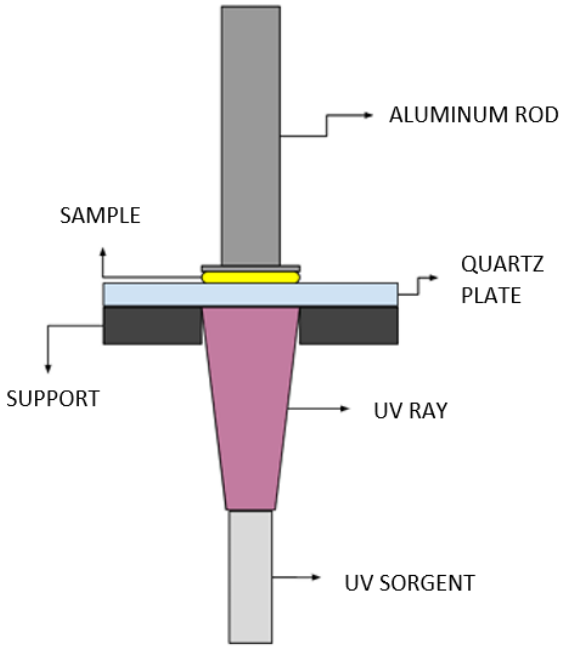

Figure 23: Schematization of the rheometer used

Table 3: Oscillatory sweep parameters used for formulations

Distance between plates (μm)	100
Frequency (Hz)	1
Oscillation amplitude (%)	1
Temperature (°C)	25
lighting of the UV lamp (s)	60

RHEOLOGY

A rheology test was conducted to observe changes in viscosity of materials. Specifically, the shear rate test was conducted where the change in viscosity (η) of the solution as a function of strain rate (γ) is measured. From the curve obtained, materials can be divided into three different categories:

- Newtonian fluids: the viscosity remains constant as the shear rate changes
- Dilatant fluids: viscosity increases as shear rate increases
- Pseudoplastic fluids: viscosity decreases as shear rate increases.

In this thesis, an Anton Paar MCR 302 rheometer with a flat plate configuration was used. The process parameters used for the shear rate test are shown in Table 4.

Table 4: Shear rate test parameters used for formulations.

Distance between plates (μm)	100
Shear Rate range (1/s)	1-1000
Temperature (°C)	25

4.3.2 STRESS RELAXATION

A stress relaxation test was conducted to verify the vitrimeric behavior of the formulations. As extensively described in Section 2.1.1 the material can be called vitrimeric if the stress relaxation follows the Maxwell equation:

$$\frac{G}{G_0} = e^{-\frac{t}{\tau*}}$$

where the relaxation time $\tau*$ is obtained when $\frac{G}{G_0} = \frac{1}{e} \approx 0{,}37$.

An Anton Paar MCR 302 rheometer with a flat plate type configuration was used to perform the test. The samples used were discs with a diameter of 25mm and a thickness of 500um. These were first preloaded with a normal force of 10N for 5 minutes at the set temperature, to allow the sample to reach the desired temperature, and then a strain of 10% was applied and the relaxation modulus over time was measured. The temperatures chosen for the tests are specifically 150°C and 170°C.

4.3.3 SWELLING AND GEL PERCENTAGE TEST

SWELLING TEST

A swelling test was conducted to evaluate the ability of the material to absorb liquids and swell.

The samples used had an average weight of about 80-90 mg, and for each formulation the test was repeated on three different samples to get statistically significant results.

Once printed, the samples were weighed to record the initial weight (m_0) and then soaked in acetone for different time intervals to record the weight gain. Specifically, the control intervals were after 1,2,3,5,10,15,20,30,60 minutes, and then up to about 90 minutes when the final weight (m_f) reached plateau.

From the data obtained, the degree of swelling S was calculated following the following formula:

$$S = \frac{m_f - m_0}{m_0} \times 100$$

GEL PERCENTAGE EVALUATION

A gel percentage test was conducted to obtain an indication of the amount of unreacted monomer at the end of the curing process. This analysis is particularly useful in the biomedical field because residual unreacted resin can cause instability or toxicity when in contact with other biological materials.

The test involves evaluating the percent weight change of a sample before and after it has been immersed for 24 hours in a solvent; to obtain a reliable measurement, after the sample is extracted, it is dried to remove the absorbed solvent. Again, three different tests were performed for each formulation to have statistical significance.

Specifically, all samples were soaked for 24 hours in acetone and allowed to dry for 48 hours before measuring the final weight.

4.3.4 DIFFERENTIAL SCANNING CALORIMETRY ANALYSYS (DSC)

A DSC analysis was conducted to investigate the thermal properties of formulations. This analysis allows measurement of the difference in heat flux associated with thermal transitions between the test sample and a reference sample when both are subjected to a controlled temperature program. From the results, it is possible to analyse the endothermic and exothermic processes in the material and draw conclusions by comparing the differences between the analyses.

The DSC was carried out with a DSC 204 F1 Phoenix machine and was designed to simulate the heat treatment undergone by materials, thus reaching 180°C, in air atmosphere.

Five heating/cooling cycles were set:

- First cycle: cooling cycle, which is used to bring the sample from room temperature to the minimum temperature from which you want to start the analysis;
- Second cycle: heating cycle, representative of the analyzed sample;
- Third cycle: cooling cycle, which is used to clear the thermal history of the material;
- Fourth cycle: heating cycle, representative of the material analyzed;
- Fifth cycle: cooling cycle which is used to bring the sample back to room temperature.

In the heating phases, the temperature was increased at a rate of 5°C/min, while in the cooling phases, the temperature was lowered at a rate of 20°C/min.

Between the end of one cycle and the beginning of the next cycle, 30-minute isotherms were set to ensure that the material reached the set temperatures. Table 5 summarized the thermal program used for all the formulations analysed.

Table 5: thermal program used for DSC

First cycle	25°C to 0°C	20°C/min
Isotherm	0°C	For 30 min
second cycle	0°C to 180°C	5°C/min
Isotherm	180°C	For 30 min
third cycle	180°C to 0°C	20°C/min
Isotherm	0°C	For 30 min
fourth cycle	0°C to 180°C	5°C/min
Isotherm	180°C	For 30 min
fifth cycle	180°C to 25°C	20°C/min

Using Netzsch Proteus Thermal Analysis software, the glass transition temperatures Tg of the analysed materials were identified.

4.3.5 FTIR-ATR SPECTROSCOPY

A measurement by IR spectroscopy was conducted to obtain information about the chemical composition of the analysed materials. IR spectroscopy is based on the principle that when a material is irradiated with monochromatic radiation belonging to the infrared range (4000-400 cm^{-1}), photons can activate vibration modes characteristic of the excited chemical bond, causing partial absorption of that radiation. It is therefore possible to obtain information about the chemical structure of the material by studying the differences between the spectra obtained.

The spectrometer FT-IR Nicolet iS50 in ATR mode was used to conduct this analysis. ATR is an analysis that allows the properties of samples to be measured only at the surface level (about 1-2 µm), so the samples used were reduced to powder or were particularly thin, so that the results could be generalized to the entire object.

The spectra obtained correspond to the average of 64 scans over a wavelength number range of 4000 to 400 cm^{-1}, with a resolution of 2.0 cm^{-1}.

4.3.6 MECHANICAL CHARACTERIZATION

Tensile tests were conducted to determine the elastic modulus value and percent elongation at break of the material, calculated from the stress-strain curves obtained.

The formulas used for obtaining the stress σ and strain ε are given below:

$$\sigma = \frac{F}{A}$$

where F is the force measured by the load cell and A indicates the useful area of the specimen (s x L) (Figure 24);

$$\varepsilon = \frac{\Delta z}{l_0} x\ 100$$

where Δz is the elongation recorded by the machine and l_0 is the measured initial length, which varies depending on how the specimen was positioned between the grips.

A tensile machine (Instron) was used with a load cell capacity of 500 N for the material before heat treatment and 10 KN for the heat-treated material, with a strain rate of 10 mm/min and test termination at specimen breakage.

The samples used were molded in the shape of a dumbbell specimens (figure 24) by the procedure described in Section 4.2.3 with a 6mm thickness and a useful cross section of 17mm length and 2mm width.

For better reliability of the results, about 10 tests were performed for each formulation considered.

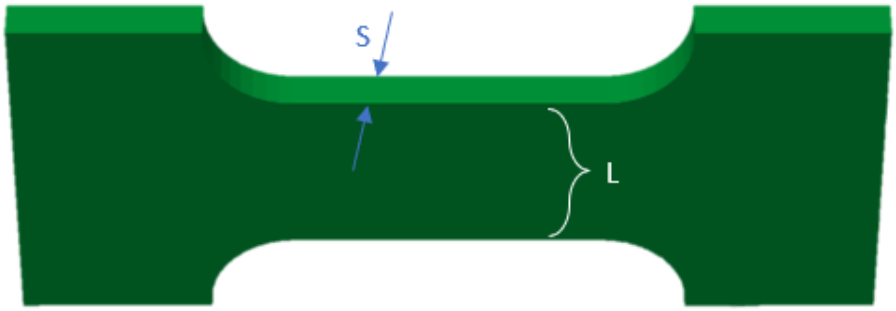

Figure 24: CAD used for tensile tests

4.3.7 SELF-HEALING TEST

Tests were conducted to see if the material had any self-healing characteristics, typical of vitrimeric materials, given by heat treatment. Specifically, tensile tests and film-making tests were conducted.

TENSILE TEST

Tensile tests were conducted in the same manner as described in Section 4.3.6 on dumbbell specimens where a hole was drilled in the centre of the useful section to simulate material failure. The CAD used to print the "broken" specimens is shown in Figure 25.

During heat treatment, the hole was filled with the missing material, and the tensile test was then done by calculating the elastic modulus of the material and comparing it with the "sound" material taken as a reference.

To confirm the results obtained, tests were also made with drilled dumbbell speciments, where the hole was not filled, used as a reference of a totally broken material.

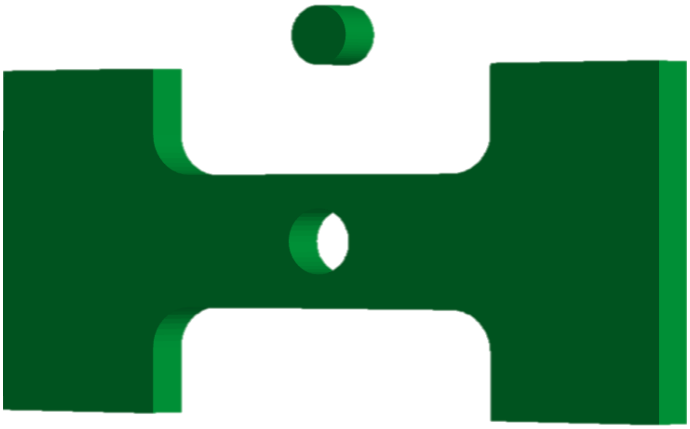

Figure 25: CAD used for tensile testing to evaluate self-healing

FILM FABBRICATION

Experimental tests were conducted to verify the possibility of creating thin films of material from fragments of the same and thus verify the ability to repair and to recycle. Specifically, a hot press as used both on pieces of material before heat treatment with a pressure of 5 tons and on pieces of material heat-treated with a pressure of 10 tons. All measurements were conducted at 150°C and 170°C.

4.3.8 3D SCANNER

A 3D scanner was used to compare the printed geometry with that obtained with CAD software and thus be able to evaluate the printing fidelity. The scanner used was the 3Shape E4 (3Shape A/S, Copenhagen, Denmark), equipped with four 5 MP cameras and with a measurement accuracy of 4 µm. Scan analysis was performed with 3Shape's Convince software.

The scanned objects were covered with a thin layer of talcum powder to reduce the reflections and glossiness of the object and not to compromise the scan. Comparison of the resulting image with the original CAD file allowed obtaining colorimetric map.

CHAPTER 5: RESULTS AND DISCUSSION

This chapter will present and analyze the results obtained from the experimental tests conducted. The objective of this thesis is the production and characterization of printable vitrimeric materials by DLP printing. The project started with the study of a synthetic vitrimer based on HPPA and GDGDA ([33]) with the intention of replacing the synthetic crosslinker with a natural crosslinker based on methacrylate cellulose to make the material more sustainable. Numerous tests were conducted to verify whether the behavior of the new vitrimer was similar to that of the original synthetic vitrimer. The experimental analyses conducted can be divided into several stages, each of which allowed specific characteristics of the material to be evaluated. Initially, preliminary rheology and photoreology tests were conducted to determine which percentage of MCC was most suitable for the production of natural vitrimer. Once the most promising percentage was identified and vitrimeric behavior was verified through stress relaxation tests, subsequent characterizations of the material were carried out, which included swelling analysis, recovery testing, DSC and IR spectroscopy, to analyze the material in detail and understand its properties and composition. Next, the mechanical properties of natural vitrimer were studied, including evaluating its self-healing and reprocessability properties.

The work was concluded by testing the printing fidelity using 3D scans of the material, to evaluate the possible use of vitrimer in the production of trabecular bone portions for testing prostheses, due to the promising mechanical characteristics in this area.

5.1 RHEOLOGY AND PHOTORHEOLOGY: CHOICE OF THE BEST FORMULATION

PHOTOREOLOGY

To study the reactivity of the formulations described in Section 4.2.2, oscillatory sweep tests were performed. The methods used are described in detail in section 4.3.1.

The obtained tests were plotted on the same graph to better perceive the comparison and shown below, in Figure 26.

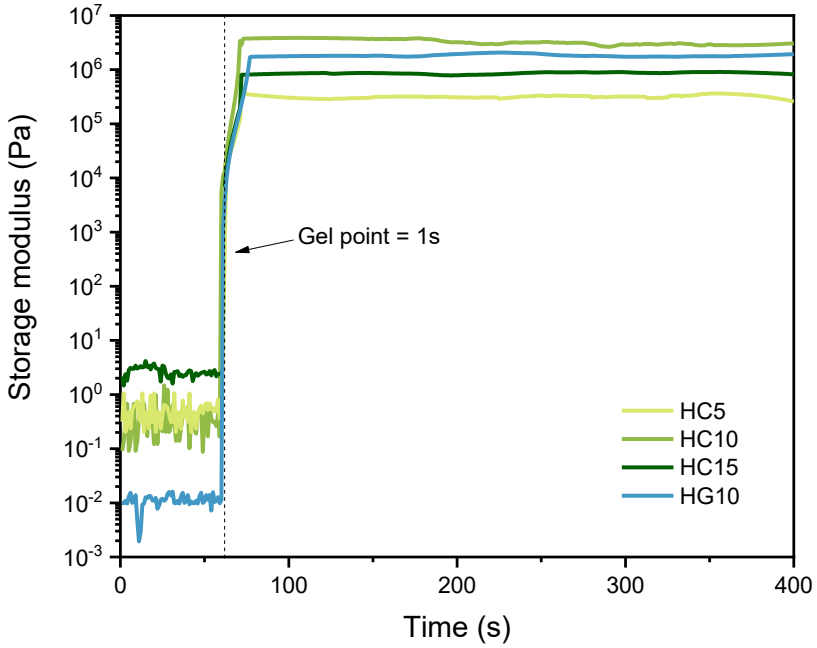

Figure 26: photoreology results

As can be seen from the graph, all formulations analysed underwent a rapid increase in storage modulus G' immediately after turning on the UV lamp and reached comparable final values.

The gel point was reached at 1 second after the lamp was turned on, and this shows a strong reactivity of all formulations, which are able to solidify in a very short time.

Specifically, if synthetic vitrimers HG10 is taken as a comparison term, the natural vitrimers that deviates the most is HC5. This could be explained by the fact that HC5 has a lower percentage of crosslinkers than the other formulations, which makes the crosslinking density lower. As a result, the polymer chains in HC5 can move more freely and the material is able to store less elastic energy during deformation.

RHEOLOGY

Shear rate tests were done to study the viscosity of the formulations, following the methods described in detail in section 4.3.1.

Figure 27 shows the obtained tests, plotted on the same graph to compare viscosities.

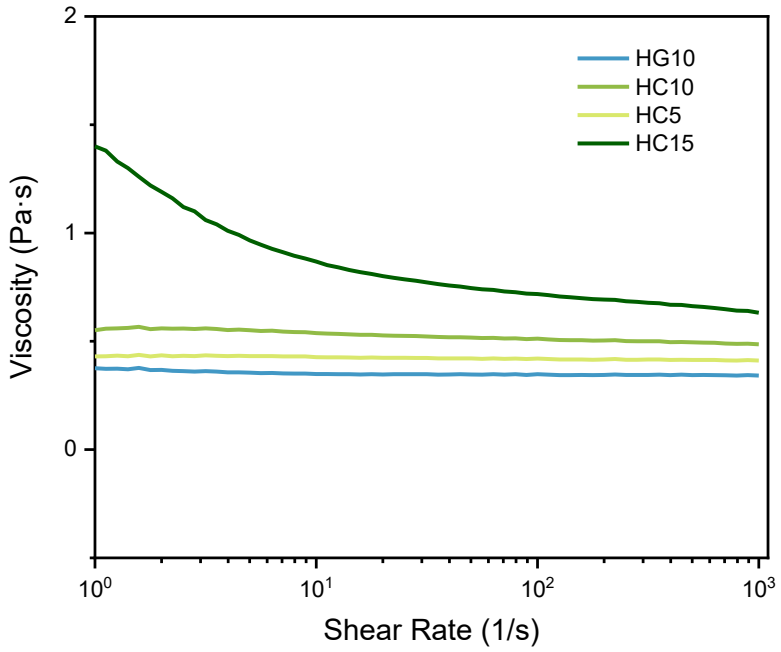

Figure 27: rheology results

As can be seen from the graph, the HC15 formulation has nonlinear behavior for shear rates between 1 and 10 1/s. This range coincides with the speeds at which the DLP printer used works, and consequently nonlinearity in this stretch can be a problem.

The nonlinear behavior could be attributed to the methacrylate cellulose powder: an excessive percentage by weight tends to cause lumps within the formulation, which are difficult to remove.

CHOICE OF FINAL FORMULATION

To continue the analysis, HC15 and HC5 formulations were excluded because for the objective of the work it is useful to have the highest possible weight percentage of methacrylate cellulose, but without having problems related to viscosity nonlinearity in the printer's range of interest. The HC10 formulation, therefore, is chosen as the final formulation for comparison with the synthetic vitrimer HG10.

5.2 STRESS RELAXATION

In order to properly study and define the behavior of the natural vitrimer HC10 chosen for comparison, stress relaxation tests were carried out, following the methods described in detail in Section 4.3.2.

Figure 28 and 29 show the tests obtained for the two materials chosen for comparison, HG10 and HC10, respectively.

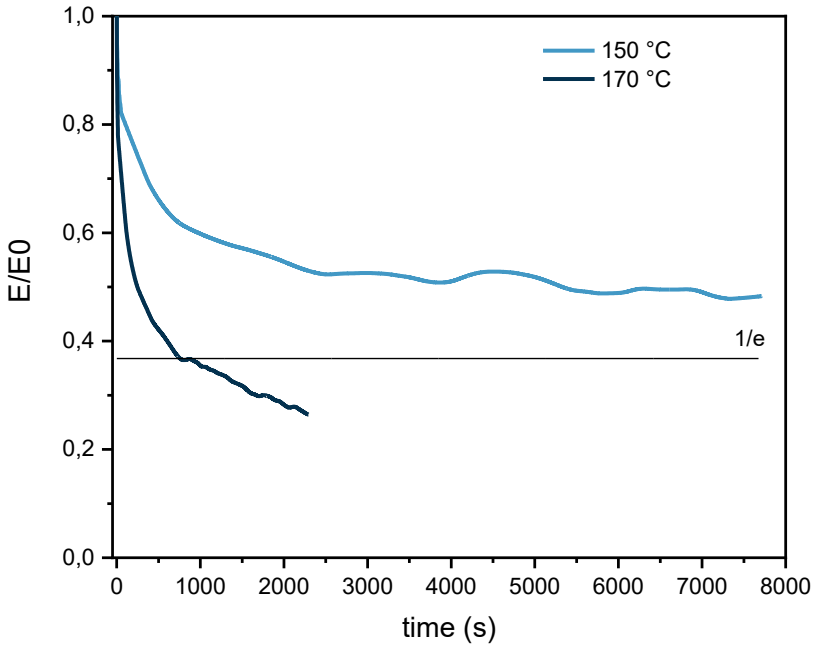

Figure 28: stress relaxation tests on HG10

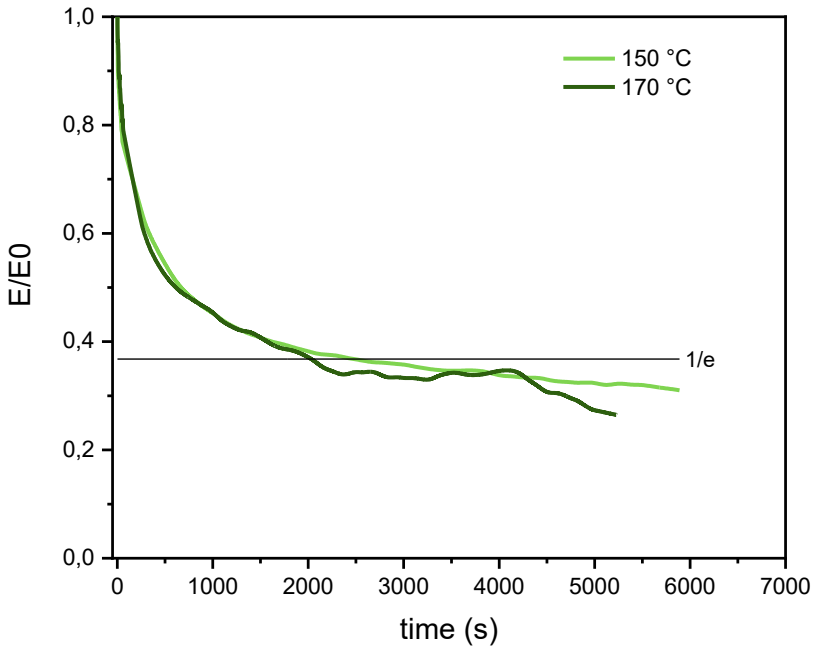

Figure 29: stress relaxation tests on HC10

A material can be called vitrimeric if the stress relaxation curves reach and exceed a horizontal asymptote of 1/e. [1]

Looking at the behavior of HG10, it can be seen that at a temperature of 150°C the material cannot be called vitrimeric: it is necessary to reach a temperature of 170°C for the stress relaxation curve to exceed the horizontal asymptote of 1/e.

If we consider the stress relaxation curves of HC10, vitrimeric behavior is already identifiable at 150°C, when after about 30 minutes from the start of the test the curve exceeds the horizontal asymptote useful for definition.

5.3 SWELLING AND GEL CONTENT TEST

SWELLING TEST

Swelling tests were conducted to study the absorption and swelling capabilities of the material. The test methods are described in detail in Section 4.3.3.

Figure 30 shows the results obtained, comparing HG10 and HC10. Both formulations reach plateau after about one hour from the start of the test.

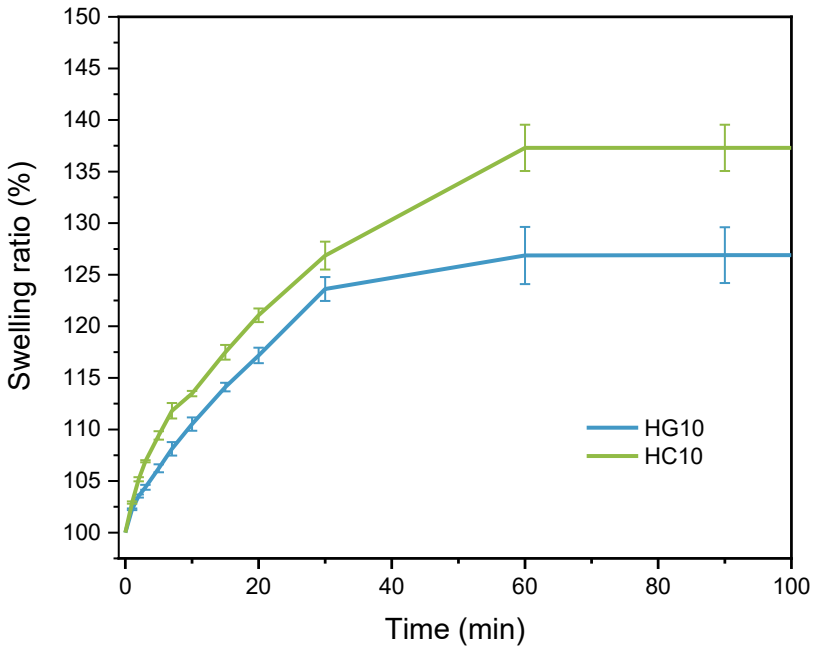

Figure 30: swelling test results

From the data obtained, it can be seen that the vitrimer with methacrylate cellulose tends to swell more. This could be due to the flexible structure of the chemical skeleton of the cellulose, which

tends to create a less dense and rigid polymerization than that created by the GDGDA synthetic crosslinker, thus allowing more solvent to enter in the polymer network.

An additional swelling test was subsequently performed on HC10 after the material underwent heat treatment at 180°C, but no significant weight gain was recorded: the material does not absorb acetone after the heating step. This can be an indication that very dense network is obtained after thermal treatment.

GEL CONTENT TEST

To analyze the percentage of material actually reacted after the curing process, gel content tests were conducted, following the methods described in detail in Section 4.3.3.

The materials studied are HG10, HC10 before heat treatment and HC10 after heat treatment, and the results obtained are shown in Table 6.

Table 6: recovery test results

RECOVERY TEST (%)	
HG10	94,9 ± 0,7
HC10	96,6 ± 0,6
HC10 TT	100 ± 0,1

From the data obtained, it can be concluded that the materials with the different crosslinkers do not show significantly different levels of crosslinking: in both vitrimers polymerization occurred successfully and most of the resin reacted, crosslinking.

After HC10 heat treatment, complete crosslinking of the material is achieved; this is due to the prolonged heating of the material that allowed the little resin that had not yet reacted to finish crosslinking properly.

5.4 DSC

To record the endothermic and exothermic processes within the HC10 vitrimer, DSC tests were conducted, following the methods described in Section 4.3.4.

Conclusions on the type of reactions occurring within the complete formulation were made starting from DSC analyses of the HPPA functional monomer alone, to which the rest of the components were added progressively. The graphs obtained are shown below.

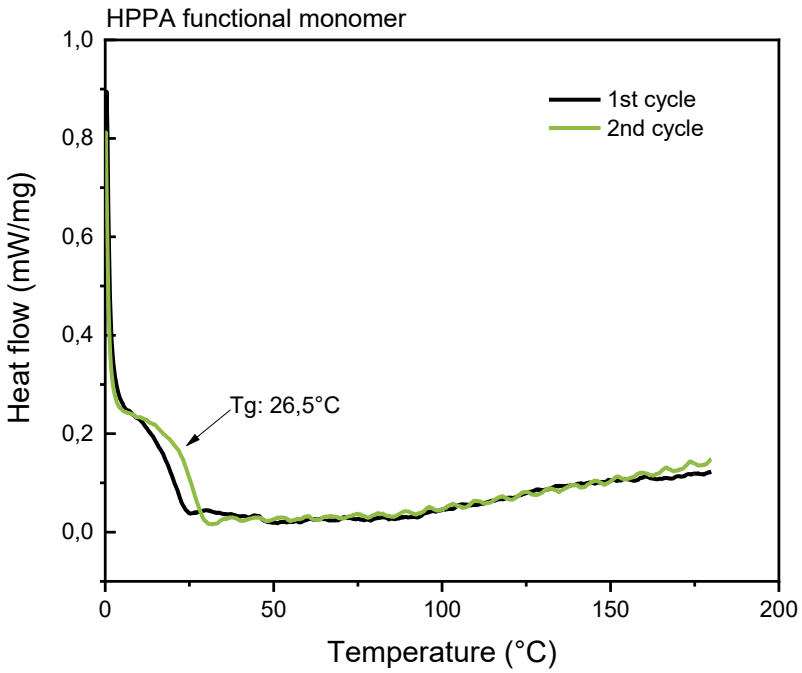

Figure 31: DSC of HPPA

DSC analysis of the functional monomer was done to calculate the glass transition temperature Tg of HPPA, which measures about 26.5 °C, and make comparisons with the Tg of the complete HC10 vitrimer formulation.

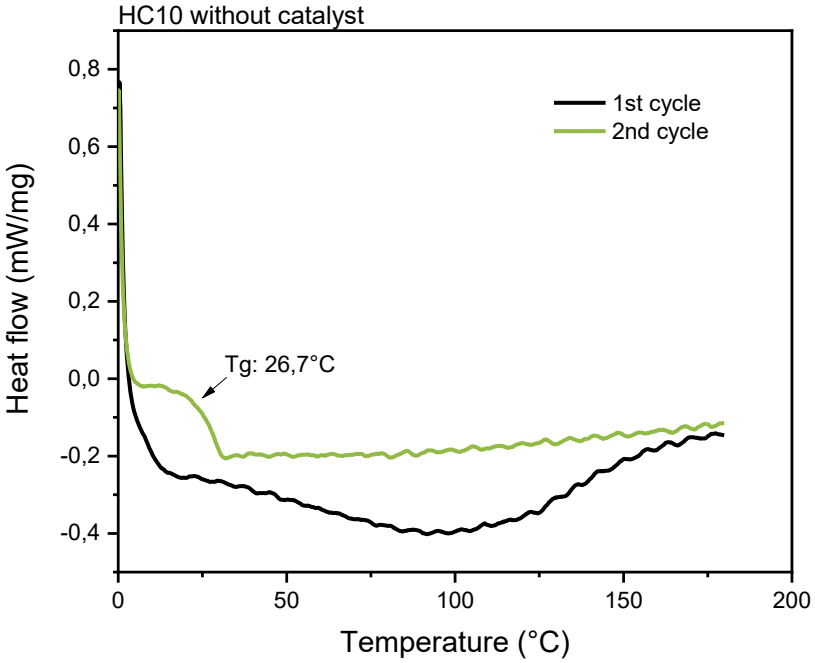

Figure 32: DSC of HC10 without catalyst

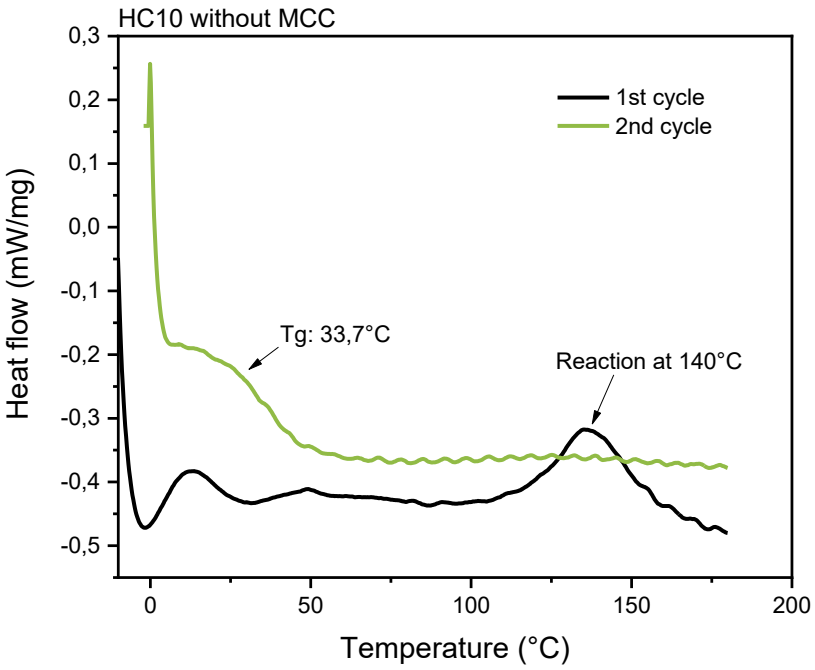

Figure 33: DSC of HC10 without MCC crosslinker

Comparing the graphs of HC10 without the methacrylate cellulose and HC10 without the catalyst, it can be seen that in the formulation where the catalyst is present there is an exothermic peak centered at 140°C, which is absent, however, in the graph where the catalyst is missing. It can therefore be assumed that between 130°C and 150°C the transesterification reaction promoted by the Miramer A99 catalyst occurs. This hypothesis is supported when considering the two newly calculated transition temperatures: in the absence of the catalyst, the Tg temperature (of about 26.7°C) does not vary significantly from that previously calculated with the functional monomer alone, while with the presence of the catalyst, the Tg increases to 33.7°C. This phenomenon could be related to an increase of cross-linking density due to transesterification reaction.

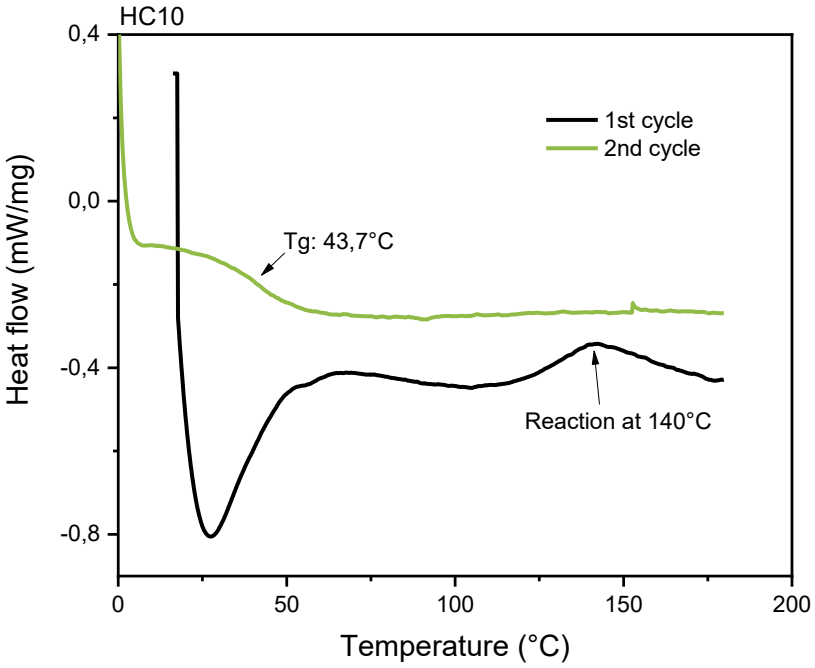

Figure 34: DSC of HC10

In the complete formulation of HC10, what was said before is confirmed; in fact, there is the peak of transesterification at 140°C and the Tg is again increased to 43.7°C confirming the hypothesis of the increase in the cross-linking density of the material given by the transesterification reaction.

Further analysis can be conducted to better investigate the mentioned aspects, including a TGA-IR analysis. This analysis could provide useful information on the chemical composition of the decomposition products during sample heating.

5.5 FTIR-ATR SPECTROSCOPY

ATR-mode tests were conducted to investigate the chemical composition of the HC10 vitrimer. The modes were described in detail in Chapter 4.3.5.

Also for this type of analysis, the spectra of the different ingredients in the formulation were compared, assuming the chemical composition by comparison. Specifically, tests were conducted on methacrylate cellulose, on HC10 without catalyst, on HC10 without crosslinker and then on the complete HC10 formulation before polymerization, after polymerization and after heat treatment.

Graphs were normalized to the peak corresponding to the vibration of the carbonyl groups, at 1720 cm^{-1}, to improve comparisons between different spectra.

The results obtained are shown below.

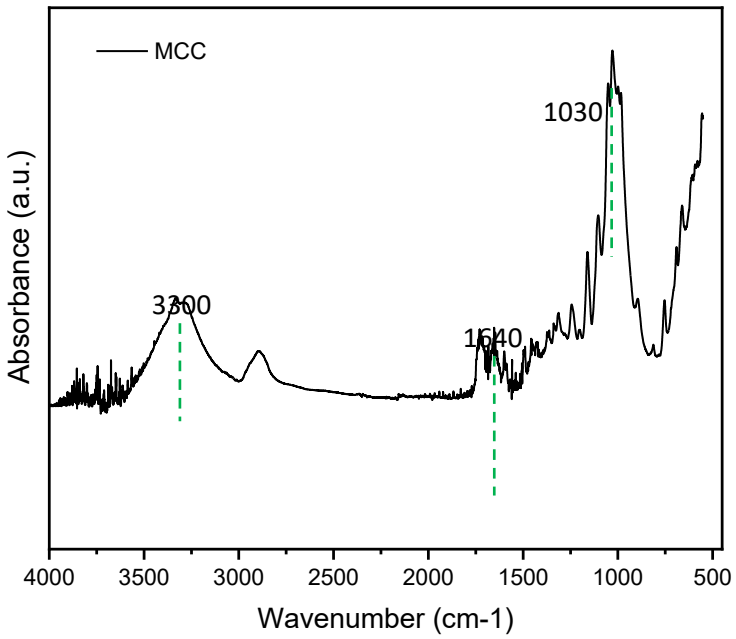

Figure 35: IR spectroscopy of MCC

From the spectroscopy analyses conducted on the methacrylate cellulose powder, three peaks of interest can be identified:

- peak at 3300 cm^{-1}: this is characteristic of the hydroxyl groups of methacrylate cellulose. The -OH groups are particularly important in the formulation because they enable the transesterification reaction. MCC was chosen as the crosslinker of the material precisely because it is rich in these groups
- -peak at 1640 cm^{-1}: this is characteristic of methacrylate groups so the functionalization of cellulose was successful.
- -peak at 1030 cm^{-1}: it is characteristic of the C-O-C ether groups typical of cellulose. In fact, methacrylate cellulose is a molecule that preserves the main skeleton of cellulose, which consists of glucose units connected by glycosidic bonds (C-O-C).

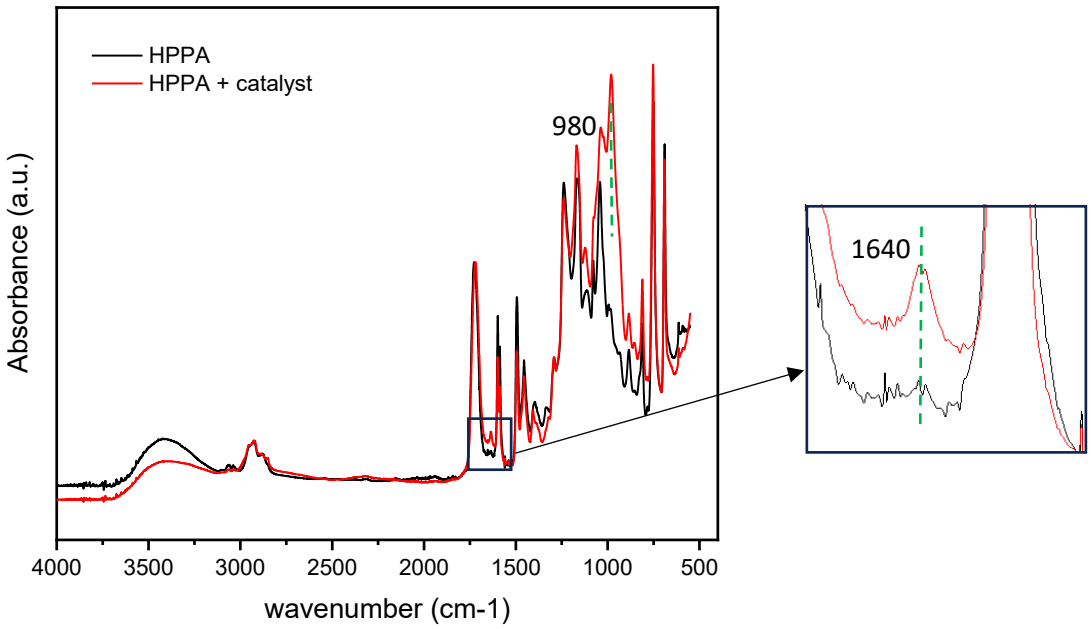

Figure 36: comparison of IR spectroscopy between HPPA and HPPA + catalyst

Comparing the spectrum obtained from the functional HPPA monomer and the monomer joined to the catalyst, two points of interest can be identified:

- Peak at 1640 cm^{-1}: it is related to the methacrylate groups of the catalyst.
- Peak at 980 cm^{-1}: is characteristic of the vibrations of the phosphate group PO4 present in the catalyst.

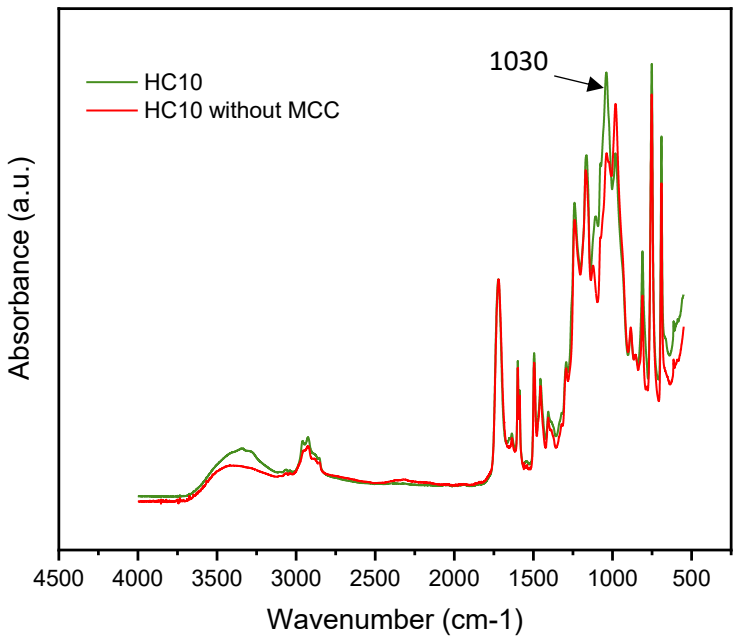

Figure 37: comparison of IR spectroscopy between HC10 and HPPA without MCC

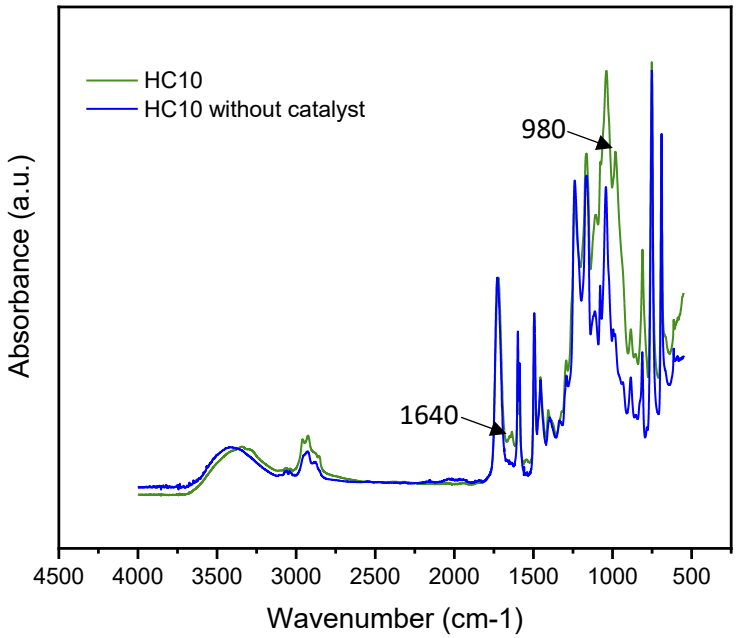

Figure 38: comparison of IR spectroscopy between HC10 and HPPA without catalyst

From the graphs obtained by subtracting methacrylate cellulose and catalyst from the HC10 formulation, respectively, the data described above can be confirmed. Specifically, when methacrylate cellulose is missing, there is a significant reduction in the peak centred at 1030 cm^{-1} that is related to the glycosidic bonds of cellulose, while in the absence of the catalyst the peak at 980 cm^{-1} of the PO4 group disappears and the peak at 1640 cm^{-1} of the methacrylate is reduced.

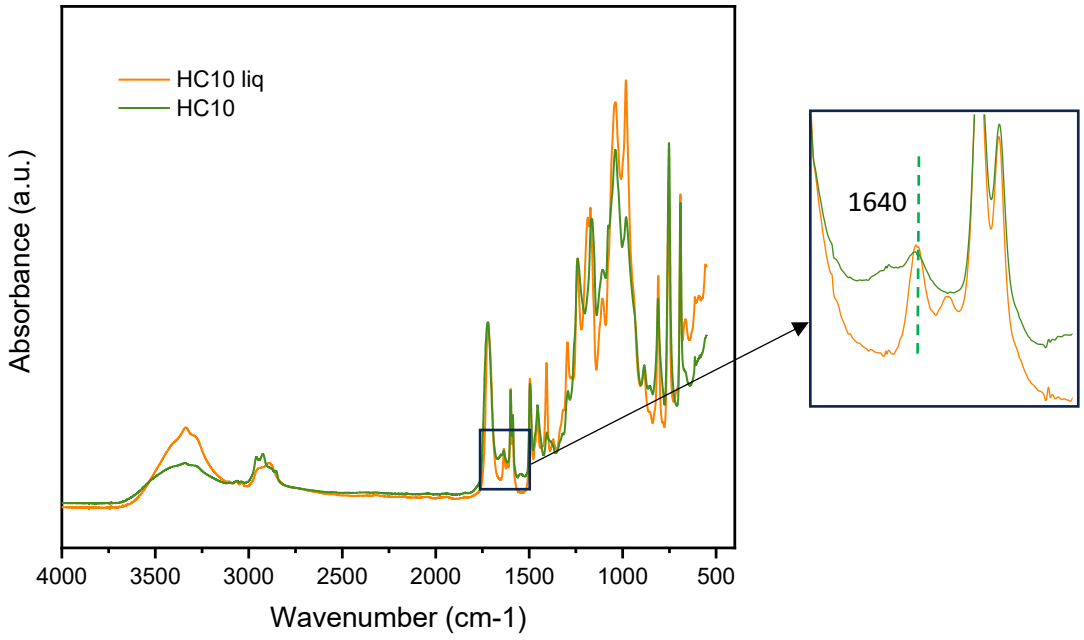

Figure 39: comparison of IR spectroscopy between liquid HC10 and polymerized HC10

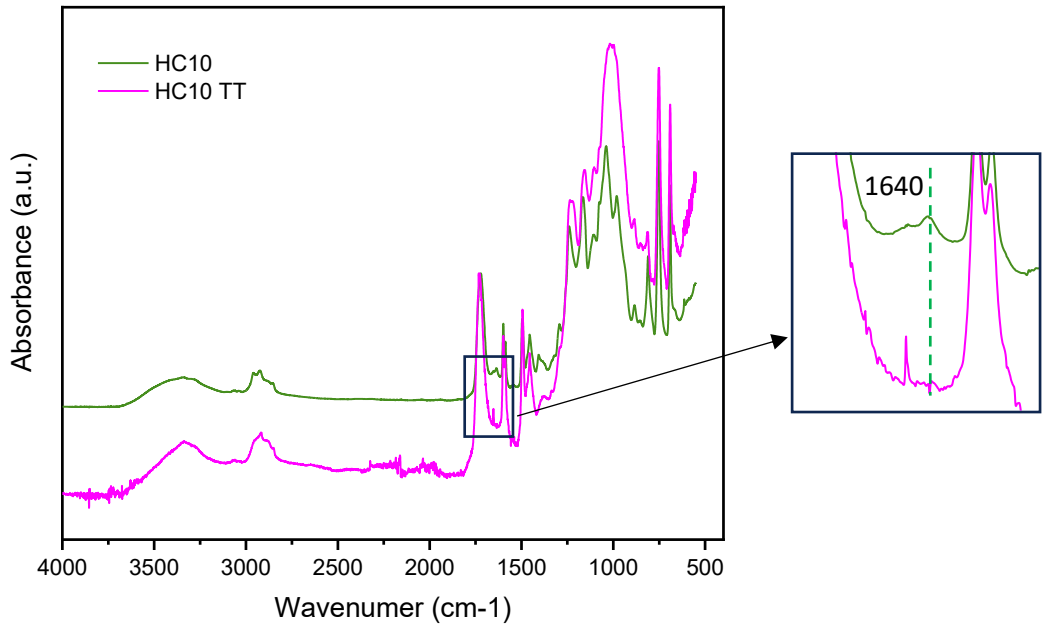

Figure 40: Comparison of IR spectroscopy between HC10 before heat treatment and after heat treatment (HC10 TT)

Comparing the various stages of the HC10 process, there are no major differences, but the progressive lowering related to the peaks of the methacrylate groups at 1640 cm^{-1} is evident, confirming the correct polymerization of the material.

5.6 TENSILE TEST

To evaluate the mechanical properties of HC10 and identify its variation during heat treatment, tensile tests were conducted on dumbbell specimens of the material before and after heat treatment (figure 41).

The specimens used were printed following the procedure described in section 4.2.3.

The obtained curves are shown together in Figure 42 to better compare the different mechanical behavior.

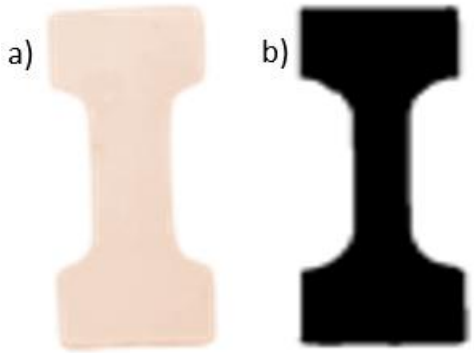

Figure 41: Tensile test specimens: a) HC10 before heat treatment, b) HC10 after heat treatment

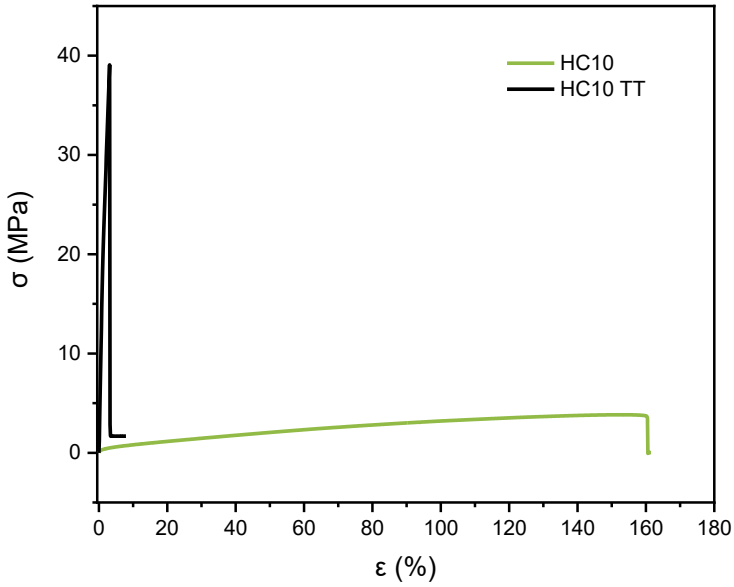

Figure 42: Tensile test results for HC10 and heat-treated HC10 (HC10 TT)

As can be seen from the data obtained, the material properties vary greatly during heat treatment. Specifically, an elastic modulus of 43 ± 4 MPa with a percent elongation of 160 % was calculated for the specimens before heat treatment, and an elastic modulus of 1815 ± 200 MPa with a percent elongation of less than 4 % after heat treatment. Heating makes the material extremely stiff and fragile.

To further visualize the drastic change in properties, a qualitative test was also conducted. Specifically, a honeycomb cube geometry was printed and used to test the material's ability to support a 200g weight before and after heat treatment. As can be seen from figure 43, the material can only hold the weight of the metal cylinder after it has been heat treated.

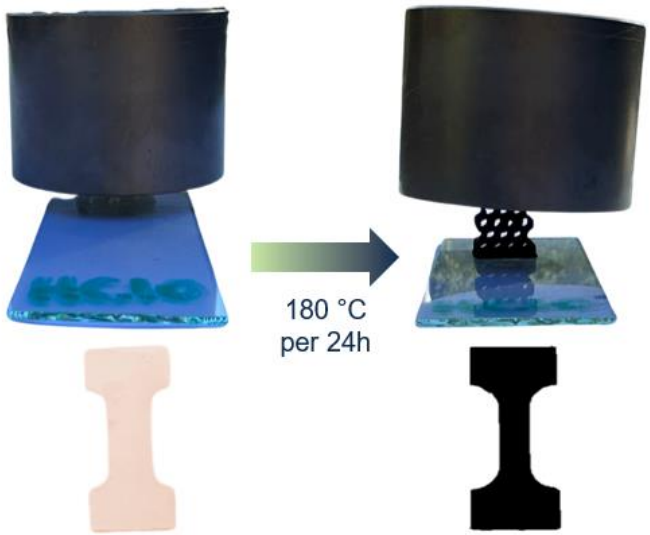

Figure 43: Qualitative test to visualize the change in mechanical properties

Interestingly, during heating, the vitrimers not only radically changes its mechanical properties but also its visual appearance, changing from a transparent white color to a deep black color. This phenomenon can be attributed to the caramelization processes of methacrylate cellulose, which begin to occur around 160°C.[40]

5.7 SELF HEALING TEST

TENSILE TEST

To evaluate the material's ability to repair itself, tensile tests were conducted on heat-treated HC10 specimens, as described in Section 4.3.7.

The samples used for the tests comparing intact material, repaired material and broken material are depicted in Figure 44. The results obtained are shown on the same graph for comparison of characteristics in Figure 45.

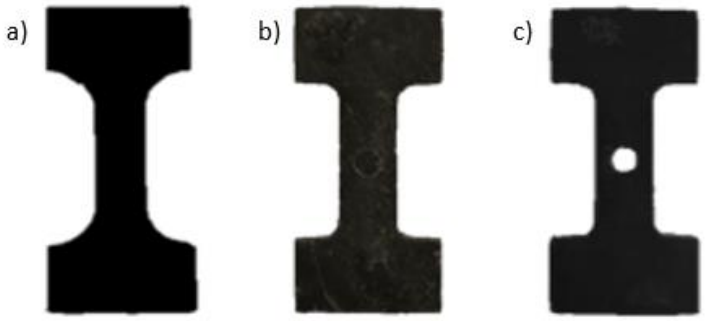

Figure 44: Self-healing test: a) intact HC10, b) repaired HC10, c) broken HC10

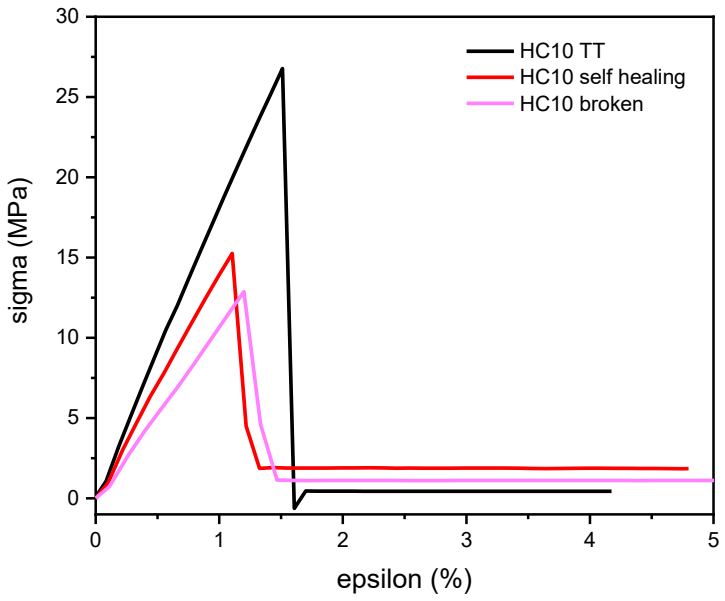

Figure 45: Comparison of tensile tests to evaluate self-healing properties

As can be seen from the curves obtained, the repaired material recovered much of the elastic modulus value of the intact material, about 78 %. This confirms that the dynamic bonds present in the starting vitrimer can indeed provide self-repair properties during heat treatment of the material. The curve of the broken vitrimer was used to confirm the self-repair of the hole made on the specimen to be repaired: the actual elastic modulus of a broken material in reality is effectively zero.

FILM FABBRICATION

Tests were conducted to assess the material's recyclability by trying to create thin films from material broken up and pressed with 5 tons at 150°C and 170°C.

Figure 46 shows the tests conducted on natural HC10 vitrimer.

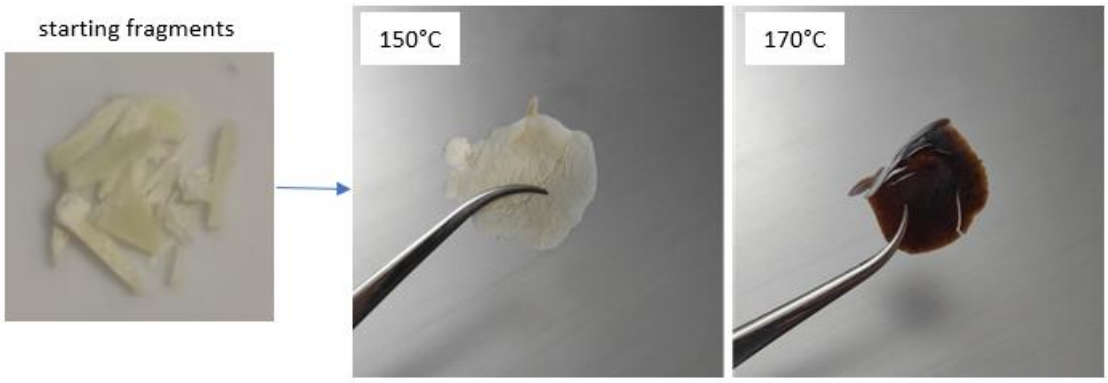

Figure 46: creation of thin films: from starting fragments to films created at 150°C and 170°C

From the results obtained, it is evident that the dynamic bonds of the material with the heat of the press were able to reorganize, allowing the creation of a thin film of material. Small cracks in the material are still present in the realized samples, but this is probably due to the placement of the initial pieces in the press too far apart.

The success of this test is also useful to confirm the correctness of the data obtained in the stress relaxation tests discussed in Chapter 5.2, where it was clearly seen that the material could be considered vitrimeric as early as 150°C. From these same tests it had been derived that the synthetic material HG10, unlike HC10, at the temperature of 150°C did not achieve the conditions necessary for the proper definition of vitrimeric material. This aspect was analysed by doing a 5-ton pressing test at 150°C. the result is shown in Figure 47, where it is evident that although a reorganization of the material is present, it is not comparable to the homogeneity obtained at 150°C with vitrimer with MCC.

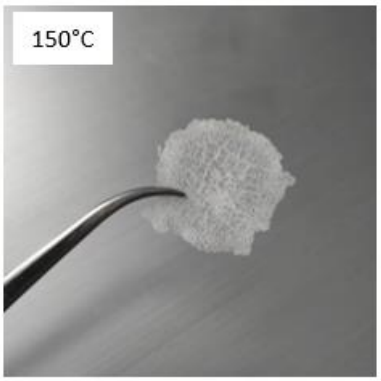

Figure 47: creation of thin films of HG10 at 150°C

5.8 3D SCANNER

To evaluate the printability of the HC10 vitrimers, small objects with complex geometries were printed; some examples are shown in Figure 48. The high resolution was confirmed by comparing a digital CAD model obtained from a 3D scan with the original CAD model designed in SolidWorks. Specifically a honeycomb CAD model was used, as this geometry allows for precise evaluation of resolution in the XY plane. Figure 49 maps the printing fidelity obtained from this comparison, showing a resolution of less than 100 µm.

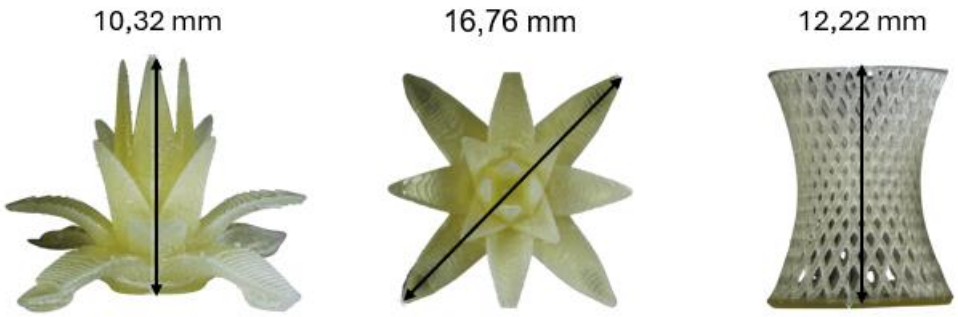

Figure 48: examples obtained with the DLP printer

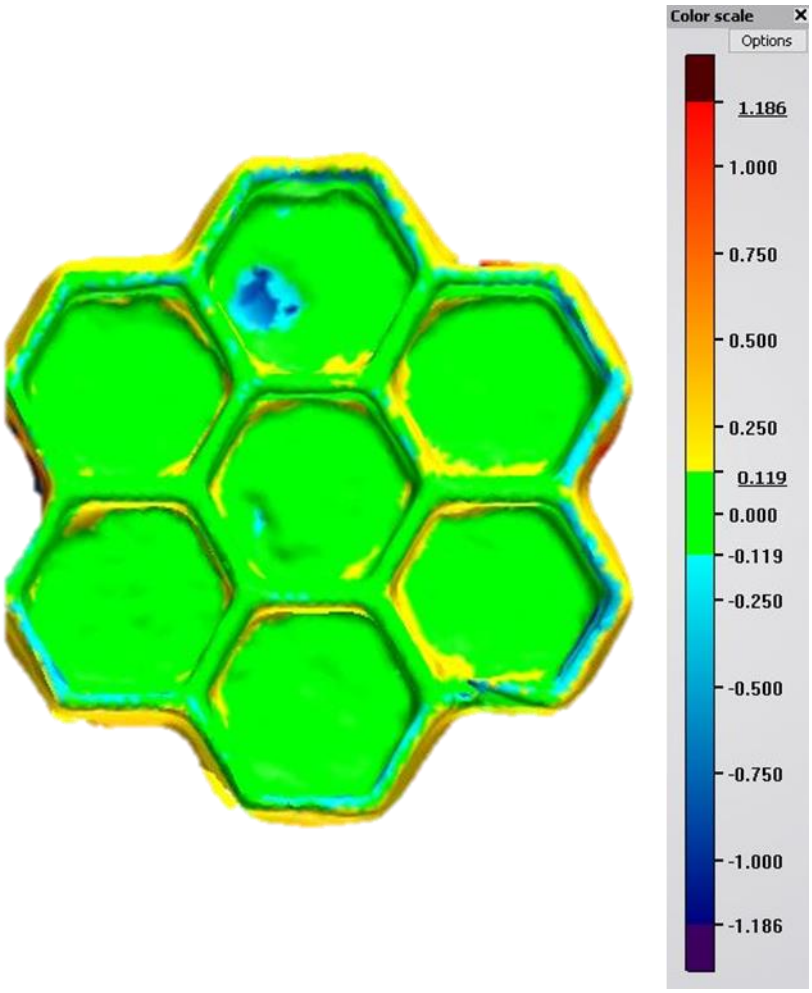

Figure 49: print fidelity map of the honeycomb structure

5.9 BIOMEDICAL APPLICATIONS OF THE MATERIAL

As widely discussed in the introductory chapters, thermosetting polymers are used in the biomedical field as they have excellent mechanical properties, thermal stability and are usually characterized by good printing resolution. One of the possible uses of thermosets in this area is the design and creation of prostheses for testing. Testing prostheses refer to prosthetic devices that are used primarily for testing and evaluation purposes, rather than for direct clinical use in patients. These prostheses are used for several specific purposes, including:

- Performance Evaluation: Test prostheses are used to evaluate the mechanical and functional performance of new materials, designs or prosthetic technologies. This includes testing for strength, durability and response under load.

- Design Optimization: Before proceeding to produce a prosthesis for clinical use, the design can be optimized through iterations based on preliminary tests. This allows you to identify and correct any design problems.
- Simulation of Clinical Conditions: These prostheses undergo simulations that replicate real clinical conditions, such as joint movement, loading forces and wear over time, to ensure that the device can function correctly in real-world situations.
- Education and Training: Test prosthetics are also useful for educational purposes, allowing doctors, surgeons and technicians to familiarize themselves with new devices and surgical techniques before using them on patients.

In this context, considering the characterization made in the previous paragraphs of the HC10 vitrimer studied, one can consider using this material as a replacement for thermosetting polymers, for the creation of test prostheses.

In fact, the analyzed vitrimer presents mechanical characteristics comparable to those of trabecular bone after thermal treatment and given the high printing fidelity verified by 3D scans, the complexity of anatomical bone parts could easily be replicated.[41]

A transition from thermosetting polymers to biobased vitrimers would therefore not only maintain the required performance but would also introduce significant advantages in terms of environmental sustainability and recyclability.

CHAPTER 6: CONCLUSION

The objective of this thesis was the development and characterization of a vitrimer with a biological crosslinker based on methacrylated cellulose, compared to a vitrimer containing a different synthetic crosslinker, in order to evaluate their similarities and differences. The methacrylated cellulose used was functionalized from cellulose derived from agro-food waste, a factor that further contributed to the sustainability of the vitrimer.

The work was divided into several phases, each contributing to outline a clear and detailed picture of the potential of the developed material.

The first part of the work focused on optimizing the composition of the vitrimer. Through preliminary rheology and photorheology tests, the optimal percentage of the natural crosslinker needed to achieve the best possible characteristics was identified. Specifically, the final formulation chosen, renamed HC10, involved the use of the functional monomer HPPA, reacted with the crosslinker MCC and the catalyst Miramer A99 in respective weight percentages of 75:10:15.

On the HC10 formulation, analyses were conducted to confirm the occurrence of transesterification through DSC and IR spectroscopy. This crucial process was demonstrated by several considerations, including the increase in the glass transition temperature of the final compound, the observation of an exothermic peak at 140°C, and the characteristic peaks of the phosphate group and methacrylates recorded in the IR tests.

Subsequently, mechanical tensile strength tests were conducted, revealing a drastic change in mechanical properties following the applied heat treatment. This behavior makes the material highly versatile, allowing its use in various operating conditions. The self-healing and reprocessability capabilities of the vitrimer were also investigated. The material can autonomously repair microfractures after heat treatment and can be reprocessed without losing its initial mechanical properties, characteristics that make it particularly suitable for applications where durability and sustainability are essential.

In the final phase of the work, the printability of the vitrimer was evaluated using Digital Light Processing (DLP) technology. The studied material guarantees a resolution of less than 100 µm and the ability to create very small and particularly complex geometries.

The combination of mechanical properties and printability of the vitrimer suggests a promising future in the biomedical field, particularly in the creation of prostheses for testing. This material could represent a valid alternative to currently used thermosetting materials, offering advantages

in terms of environmental sustainability thanks to the use of a natural crosslinker and the ability to repair and to reuse the material itself.

Certainly, there are still many aspects to explore. Regarding future work, it is planned to deepen the study of the transesterification reaction of the material through Thermogravimetric Analysis coupled with Infrared Spectroscopy (TGA-IR), which could provide information on the chemical composition of the decomposition products during sample heating and on the caramelization processes, which currently prevent the complete self-repair of a thermally treated sample. Additionally, always with a view to greater sustainability, it would be useful to verify whether and how the mechanical characteristics change after a reduced heat treatment of just a few hours, rather than prolonged for an entire day. These studies could provide further insights into the thermal and chemical behavior of the vitrimer, opening new possibilities for application and improvement of its performance.

REFERENCES

[1] M. A. Lucherelli, A. Duval, and L. Avérous, “Biobased vitrimers: Towards sustainable and adaptable performing polymer materials,” Apr. 01, 2022, *Elsevier Ltd*. doi: 10.1016/j.progpolymsci.2022.101515.

[2] J. Massy, “Thermoplastic and Thermosetting Polymers,” in *SpringerBriefs in Materials*, Springer, 2017, pp. 19–26. doi: 10.1007/978-3-319-54831-9_5.

[3] V. Schenk, K. Labastie, M. Destarac, P. Olivier, and M. Guerre, “Vitrimer composites: current status and future challenges,” Sep. 23, 2022, *Royal Society of Chemistry*. doi: 10.1039/d2ma00654e.

[4] B. Krishnakumar, R. V. S. P. Sanka, W. H. Binder, V. Parthasarthy, S. Rana, and N. Karak, “Vitrimers: Associative dynamic covalent adaptive networks in thermoset polymers,” Apr. 01, 2020, *Elsevier B.V.* doi: 10.1016/j.cej.2019.123820.

[5] W. Denissen, J. M. Winne, and F. E. Du Prez, “Vitrimers: Permanent organic networks with glass-like fluidity,” Jan. 01, 2016, *Royal Society of Chemistry*. doi: 10.1039/c5sc02223a.

[6] S. Bose, “Upcycling acrylonitrile-butadiene-styrene Vitrimer ‘in melt’ using a dynamic crosslinker,” 2023, doi: 10.21203/rs.3.rs-3618604/v1.

[7] S. Dhers, G. Vantomme, and L. Avérous, “A fully bio-based polyimine vitrimer derived from fructose,” *Green Chemistry*, vol. 21, no. 7, pp. 1596–1601, 2019, doi: 10.1039/c9gc00540d.

[8] J. Zheng *et al.*, “Vitrimers: Current research trends and their emerging applications,” Dec. 01, 2021, *Elsevier B.V.* doi: 10.1016/j.mattod.2021.07.003.

[9] A. Kumar and L. A. Connal, “Biobased Transesterification Vitrimers,” Apr. 01, 2023, *John Wiley and Sons Inc*. doi: 10.1002/marc.202200892.

[10] S. Zhang *et al.*, “Preparation of a lignin-based vitrimer material and its potential use for recoverable adhesives,” *Green Chemistry*, vol. 20, no. 13, pp. 2995–3000, 2018, doi: 10.1039/c8gc01299g.

[11] C. Hao *et al.*, “A High-Lignin-Content, Removable, and Glycol-Assisted Repairable Coating Based on Dynamic Covalent Bonds,” *ChemSusChem*, vol. 12, no. 5, pp. 1049–1058, Mar. 2019, doi: 10.1002/cssc.201802615.

[12] H. Memon *et al.*, “Vanillin-Based Epoxy Vitrimer with High Performance and Closed-Loop Recyclability,” *Macromolecules*, vol. 53, no. 2, pp. 621–630, Jan. 2020, doi: 10.1021/acs.macromol.9b02006.

[13] J. Wu, X. Yu, H. Zhang, J. Guo, J. Hu, and M.-H. Li, “Fully Biobased Vitrimers from Glycyrrhizic Acid and Soybean Oil for Self-Healing, Shape Memory, Weldable, and Recyclable Materials,” *ACS Sustain Chem Eng*, vol. 8, no. 16, pp. 6479–6487, Apr. 2020, doi: 10.1021/acssuschemeng.0c01047.

[14] X. Yang, L. Guo, X. Xu, S. Shang, and H. Liu, “A fully bio-based epoxy vitrimer: Self-healing, triple-shape memory and reprocessing triggered by dynamic covalent bond exchange,” *Mater Des*, vol. 186, Jan. 2020, doi: 10.1016/j.matdes.2019.108248.

[15] W. Zhao *et al.*, “Vitrimer-Cellulose Paper Composites: A New Class of Strong, Smart, Green, and Sustainable Materials,” *ACS Appl Mater Interfaces*, vol. 11, no. 39, pp. 36090–36099, Oct. 2019, doi: 10.1021/acsami.9b11991.

[16] C. Li, B. Ju, and S. Zhang, “Construction of a new green vitrimer material: introducing dynamic covalent bond into carboxymethyl cellulose,” *Cellulose*, vol. 28, no. 5, pp. 2879–2888, Mar. 2021, doi: 10.1007/s10570-021-03763-4.

[17] J. M. Capannelli, S. Dalle Vacche, A. Vitale, K. Bouzidi, D. Beneventi, and R. Bongiovanni, “A biobased epoxy vitrimer/cellulose composite for 3D printing by Liquid Deposition Modelling,” *Polym Test*, vol. 127, Oct. 2023, doi: 10.1016/j.polymertesting.2023.108172.

[18] J. Zheng *et al.*, “Vitrimers: Current research trends and their emerging applications,” Dec. 01, 2021, *Elsevier B.V.* doi: 10.1016/j.mattod.2021.07.003.

[19] X. Xia, P. Rao, J. Yang, M. P. Ciamarra, and R. Ni, “Entropy-Driven Thermo-gelling Vitrimer,” *JACS Au*, vol. 2, no. 10, pp. 2359–2366, Oct. 2022, doi: 10.1021/jacsau.2c00425.

[20] M. Layani, X. Wang, and S. Magdassi, “Novel Materials for 3D Printing by Photopolymerization,” Oct. 11, 2018, *Wiley-VCH Verlag*. doi: 10.1002/adma.201706344.

[21] M. N. Nadagouda, V. Rastogi, and M. Ginn, “A review on 3D printing techniques for medical applications,” Jun. 01, 2020, *Elsevier Ltd*. doi: 10.1016/j.coche.2020.05.007.

[22] S. Guessasma, W. Zhang, J. Zhu, S. Belhabib, and H. Nouri, “Challenges of additive manufacturing technologies from an optimisation perspective,” *International Journal for Simulation and Multidisciplinary Design Optimization*, vol. 6, p. A9, 2015, doi: 10.1051/smdo/2016001.

[23] M. Lang, S. Hirner, F. Wiesbrock, and P. Fuchs, “A Review on Modeling Cure Kinetics and Mechanisms of Photopolymerization,” *Polymers (Basel)*, vol. 14, no. 10, May 2022, doi: 10.3390/polym14102074.

[24] S. K. Paral, D. Z. Lin, Y. L. Cheng, S. C. Lin, and J. Y. Jeng, “A Review of Critical Issues in High-Speed Vat Photopolymerization,” Jun. 01, 2023, *MDPI*. doi: 10.3390/polym15122716.

[25] A. Bagheri and J. Jin, “Photopolymerization in 3D Printing,” Apr. 12, 2019, *American Chemical Society*. doi: 10.1021/acsapm.8b00165.

[26] Y. Li, Q. Mao, J. Yin, Y. Wang, J. Fu, and Y. Huang, “Theoretical prediction and experimental validation of the digital light processing (DLP) working curve for photocurable materials,” *Addit Manuf*, vol. 37, Jan. 2021, doi: 10.1016/j.addma.2020.101716.

[27] J. Gong *et al.*, “Digital light processing (DLP) in tissue engineering: from promise to reality, and perspectives,” Nov. 01, 2022, *Institute of Physics*. doi: 10.1088/1748-605X/ac96ba.

[28] C. Schmidleithner and D. M. Kalaskar, “Stereolithography,” in *3D Printing*, InTech, 2018. doi: 10.5772/intechopen.78147.

[29] A. Salas, M. Zanatta, V. Sans, and I. Roppolo, “Chemistry in light-induced 3D printing,” *ChemTexts*, vol. 9, no. 1, Feb. 2023, doi: 10.1007/s40828-022-00176-z.

[30] C. C. Wang, J. Y. Chen, and J. Wang, “The selection of photoinitiators for photopolymerization of biodegradable polymers and its application in digital light processing additive manufacturing,” *J Biomed Mater Res A*, vol. 110, no. 1, pp. 204–216, Jan. 2022, doi: 10.1002/jbm.a.37277.

[31] S. Grauzeliene, M. Kastanauskas, V. Talacka, and J. Ostrauskaite, “Photocurable Glycerol- and Vanillin-Based Resins for the Synthesis of Vitrimers,” *ACS Appl Polym Mater*, vol. 4, no. 8, pp. 6103–6110, Aug. 2022, doi: 10.1021/acsapm.2c00914.

[32] sigma aldrich, “Chemical structure of 2-hydroxy-3-phenoxypropyl acrylate (HPPA) .” Accessed: Jul. 13, 2024. [Online]. Available: https://www.sigmaaldrich.com/IT/it/search/2-hydroxy-3-phenoxypropyl-acrylate-(hppa?focus=products&page=1&perpage=30&sort=relevance&term=2-Hydroxy-3-phenoxypropyl%20acrylate%20%28HPPA&type=product

[33] E. Rossegger *et al.*, “High resolution additive manufacturing with acrylate based vitrimers using organic phosphates as transesterification catalyst,” *Polymer (Guildf)*, vol. 221, Apr. 2021, doi: 10.1016/j.polymer.2021.123631.

[34] sigma aldrich, “Chemical structure of Glycerol 1,3-diglycerolate diacrylate (GDGDA).” Accessed: Jul. 13, 2024. [Online]. Available: https://www.sigmaaldrich.com/IT/it/search/glycerol-1%2C3-diglycerolate-diacrylate-(gdgda)?focus=products&page=1&perpage=30&sort=relevance&term=Glycerol%201%2C3-diglycerolate%20diacrylate%20%28GDGDA%29&type=product

[35] G. Lupidi, G. Pastore, E. Marcantoni, and S. Gabrielli, “Recent Developments in Chemical Derivatization of Microcrystalline Cellulose (MCC): Pre-Treatments, Functionalization, and Applications,” Mar. 01, 2023, *MDPI*. doi: 10.3390/molecules28052009.

[36] I. Cazin *et al.*, “Digital light processing 3D printing of dynamic magneto-responsive thiol-acrylate composites,” *RSC Adv*, vol. 13, no. 26, pp. 17536–17544, Jun. 2023, doi: 10.1039/d3ra02504g.

[37] sigma aldrich, “chemical structure of Phenylbis (2,4,6-trimethylbenzoyl) phosphine oxide (BAPO).” Accessed: Jul. 13, 2024. [Online]. Available: https://www.sigmaaldrich.com/IT/it/search/bapo?focus=products&page=1&perpage=30&sort=relevance&term=bapo&type=product

[38] M. C. Cabua *et al.*, “Microcrystalline Cellulose from Aloe Plant Waste as a Platform for Green Materials: Preparation, Chemical Functionalization, and Application in 3D Printing,” *ACS Appl Polym Mater*, 2024, doi: 10.1021/acsapm.4c00409.

[39] Asiga, “Asiga MAX UVX27 printer .” Accessed: Jul. 14, 2024. [Online]. Available: https://www.asiga.com/max-x/

[40] “Ella Tirronen Brightness measurement of cellulosic materials.”

[41] D. Wu, P. Isaksson, S. J. Ferguson, and C. Persson, “Young’s modulus of trabecular bone at the tissue level: A review,” Sep. 15, 2018, *Acta Materialia Inc*. doi: 10.1016/j.actbio.2018.08.001.